Quiz

- Range of Size of Galaxies?
- What are the 2 main types of galaxies?
- What dynamical tracers in galaxies?
- What dynamical measure to measure the mass of disk galaxies? Of elliptical galaxies?
- What is the relation between halo mass and stellar mass?
- What does this relation tell us about star formation?

Gravitational Lensing - 1

Jean-Paul KNEIB

Outline

- Introduction of gravitational (strong) lensing
- A brief history & key observations
- Strong lensing on galaxy & clusters scale
- Basics of weak lensing

Very First Ideas and Measurements

1915: Einstein: General Relativity, one of the test is the deflection of light (twice larger than the Newtonian theory or 1.75 arcsec)

1919: Eddington: first measure of the deflection of light by the Sun during a solar eclipse: observations favors GR theory of Einstein

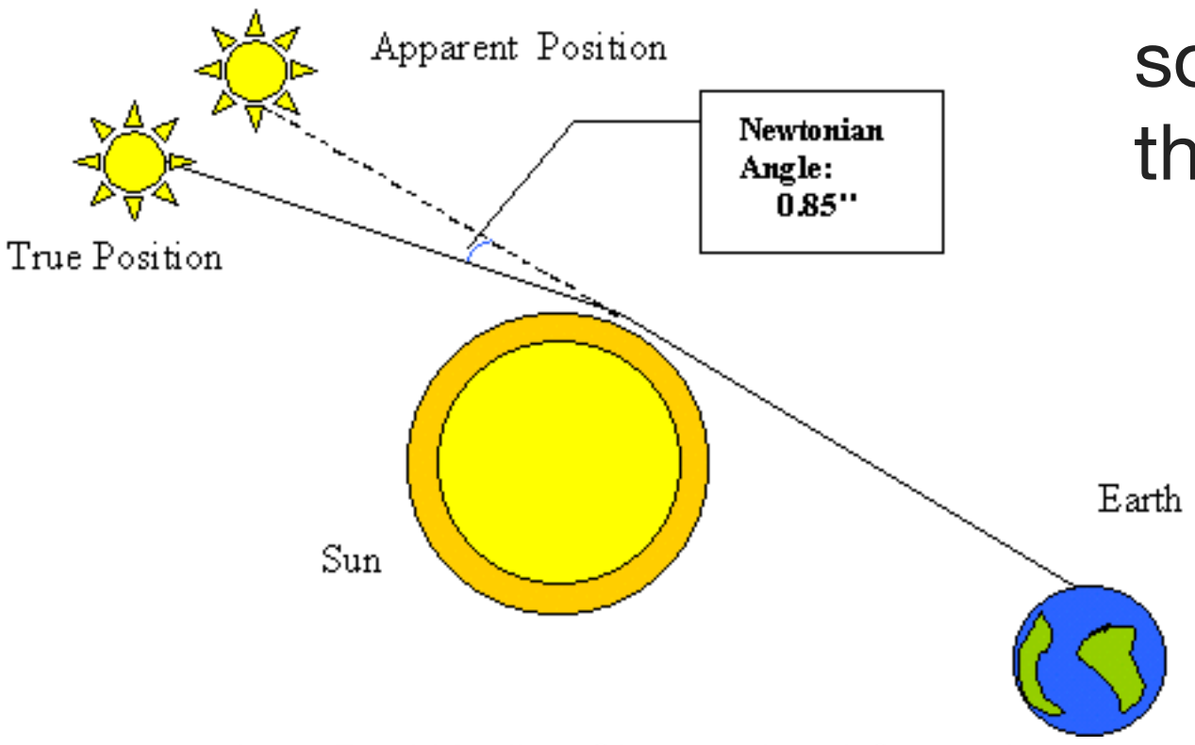

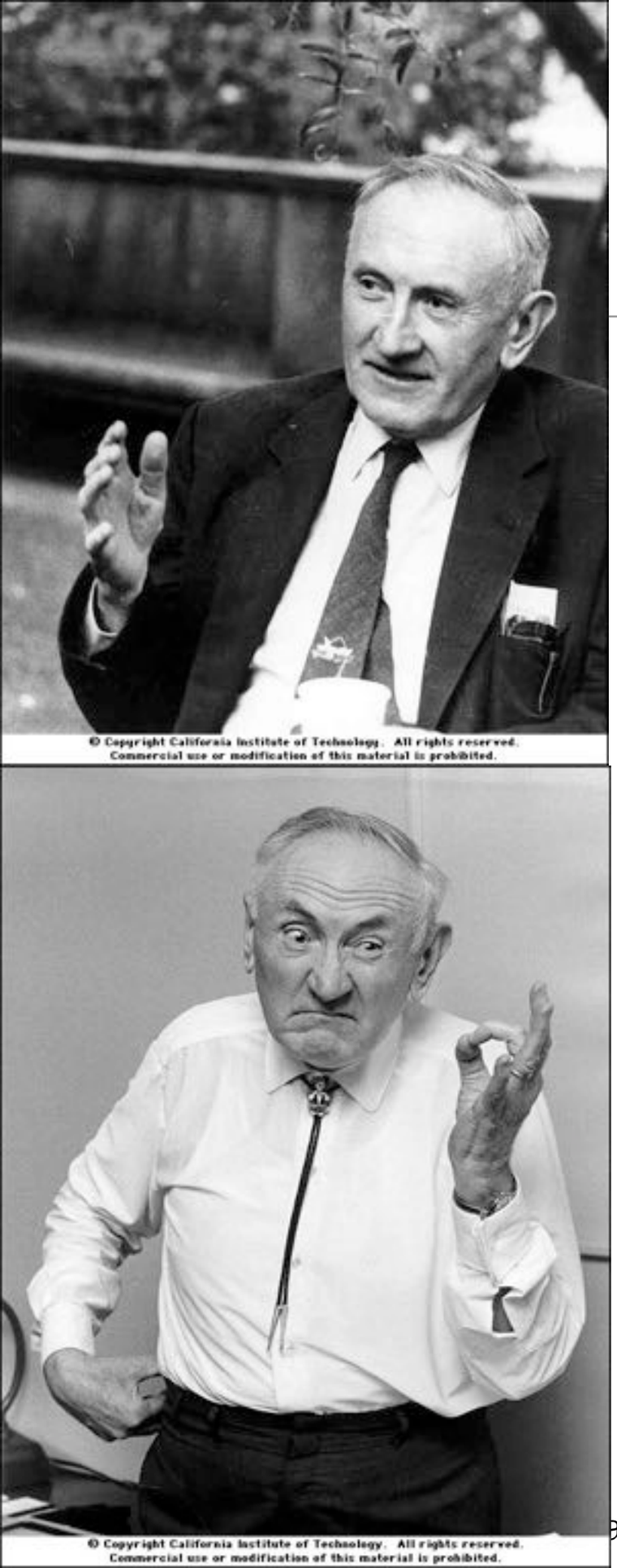

Zwicky's vision of gravitational lensing

- 1933: Zwicky "discovered" DM in Coma cluster
- 1937: Zwicky's "vision": observation of gravitational lensing (by clusters) should allow to probe:
  - the Dark Matter distribution
  - study distant galaxies thanks to the magnification effects

Nebulae as Gravitational Lenses

Einstein recently published[1] some calculations concerning a suggestion made by R. W. Mandl, namely, that a star B may act as a "gravitational lens" for light coming from another star A which lies closely enough on the line of sight behind B. As Einstein remarks the chance to observe this effect for stars is extremely small.

Last summer Dr. V. K. Zworykin (to whom the same idea had been suggested by Mr. Mandl) mentioned to me the possibility of an image formation through the action of gravitational fields. As a consequence I made some calculations which show that extragalactic *nebulae* offer a much better chance than *stars* for the observation of gravitational lens effects.

In the first place some of the massive and more concentrated nebulae may be expected to deflect light by as much as half a minute of arc. In the second place nebulae, in contradistinction to stars, possess apparent dimensions which are resolvable to very great distances.

Suppose that a distant globular nebula A whose diameter is 2ξ lies at a distance, a, which is great compared with the distance D of a nearby nebula B which lies exactly in front of A. The image of A under these circumstances is a luminous ring whose average apparent radius is $\beta=(\gamma_0 r_0'/D)^{\frac{1}{2}}$, where γ_0 is the angle of deflection for light passing at a distance r_0 from B. The apparent width of the ring is $\Delta\beta=\xi/a$. The apparent total brightness of this luminous ring is q times greater than the brightness of the direct image of A. In our special case $q=2la/\xi D$, with $l=(\gamma_0 r_0 D)^{\frac{1}{2}}$. In actual cases the factor q may be as high as $q=100$, corresponding to an increase in brightness of five magnitudes. The surface brightness remains, of course, unchanged.

The discovery of images of nebulae which are formed through the gravitational fields of nearby nebulae would be of considerable interest for a number of reasons.

(1) It would furnish an additional test for the general theory of relativity.

(2) It would enable us to see nebulae at distances greater than those ordinarily reached by even the greatest telescopes. Any such *extension* of the known parts of the universe promises to throw very welcome new light on a number of cosmological problems.

(3) The problem of determining nebular masses at present has arrived at a stalemate. The mass of an average nebula until recently was thought to be of the order of $M_N=10^9\,M_\odot$, where $M_\odot$ is the mass of the sun. This estimate is based on certain deductions drawn from data on the intrinsic brightness of nebulae as well as their spectrographic rotations. Some time ago, however, I showed[2] that a straightforward application of the virial theorem to the great cluster of nebulae in Coma leads to an average nebular mass four hundred times greater than the one mentioned, that is, $M_N'=4\times10^{11}M_\odot$. This result has recently been verified by an investigation of the Virgo cluster.[3] Observations on the deflection of light around nebulae may provide the most direct determination of nebular masses and clear up the above-mentioned discrepancy.

A detailed account of the problems sketched here will appear in *Helvetica Physica Acta*.

F. ZWICKY

Norman Bridge Laboratory,
California Institute of Technology,
Pasadena, California,
January 14, 1937.

[1] A. Einstein, Science **84**, 506 (1936).
[2] F. Zwicky, Helv. Phys. Acta **6**, 124 (1933).
[3] Sinclair Smith, Astrophys. J. **83**, 23 (1936).

Emergence of Low En

In some experiments rec
protons in alpha-particle in
studied. In several cases t
that protons of relatively
considerable numbers. Thu

$Al^{27}+H$
$P^{31}+H$
$Cl^{35}+H$
$Ca^{40}+H$

a group of protons of maxi
and the yield is in general la
total number of protons em
range 10 cm are observed w
the probability of emission
these low energy protons ge

In recent experiments in
curve for the emission of ne
particle bombardment has
radius found to be 7.3×10
Bethe's revised radii for the
be taken as a basis for calc
Si^{30}, S^{34}, A^{38}, Ca^{42} and Sc^{45}. (
experiments) indicates, if an
found in this way. In Table
lated, together with the heig
barriers and the range of a
them. It will be seen that in
observed ranges are smalle
barrier. It therefore appear
significant conclusions from
barriers to emerging protons
posite nucleus containing th
proton has a finite lifetime
proton to leak through the ba
in accordance with Bohr's

TA

Product Nucleus	Nuclear Radius ($\times10^{13}$cm)	Pro Bar He (M
Si^{30}	6.7	3
S^{34}	6.9	3
A^{38}	7.2	3
Ca^{42}	7.4	3
Sc^{45}	7.5	4

Zwicky, 1937

The discovery of images of nebulae which are formed through the gravitational fields of nearby nebulae would be of considerable interest for a number of reasons.

(1) It would furnish an additional test for the general theory of relativity.

(2) It would enable us to see nebulae at distances greater than those ordinarily reached by even the greatest telescopes. Any such *extension* of the known parts of the universe promises to throw very welcome new light on a number of cosmological problems.

(3) The problem of determining nebular masses at present has arrived at a stalemate. The mass of an average nebula until recently was thought to be of the order of $M_N=10^9\,M_\odot$, where $M_\odot$ is the mass of the sun. This estimate is based on certain deductions drawn from data on the intrinsic brightness of nebulae as well as their spectrographic rotations. Some time ago, however, I showed[2] that a straightforward application of the virial theorem to the great cluster of nebulae in Coma leads to an average nebular mass four hundred times greater than the one mentioned, that is, $M_N'=4\times10^{11}M_\odot$. This result has recently been verified by an investigation of the Virgo cluster.[3] Observations on the deflection of light around nebulae may provide the most direct determination of nebular masses and clear up the above-mentioned discrepancy.

1979

... discovery of *a the first double quasar:* an illusion created by gravity or physical twins?

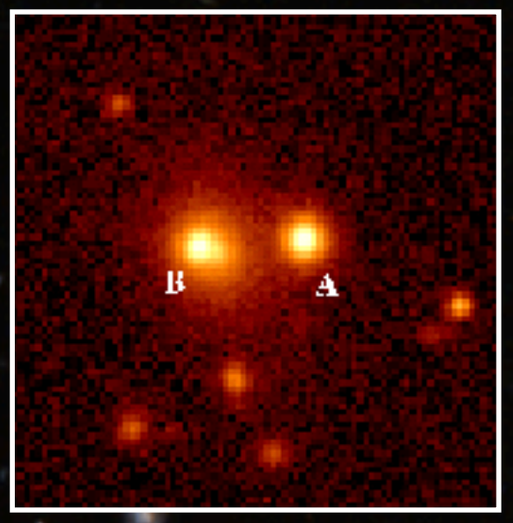

Twin Quasars

Double Quasar seen with the Hubble Space Telescope

Light curve of the double quasar and time delay

Hainline et al. (2012)

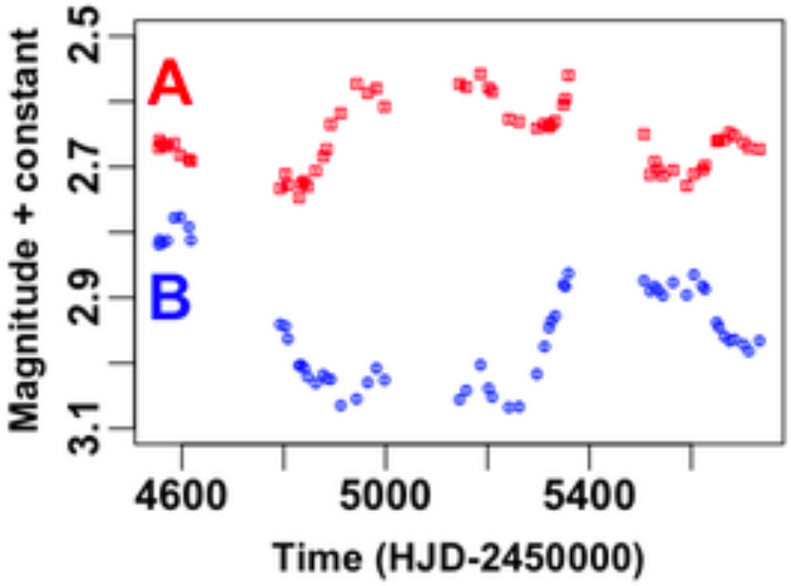

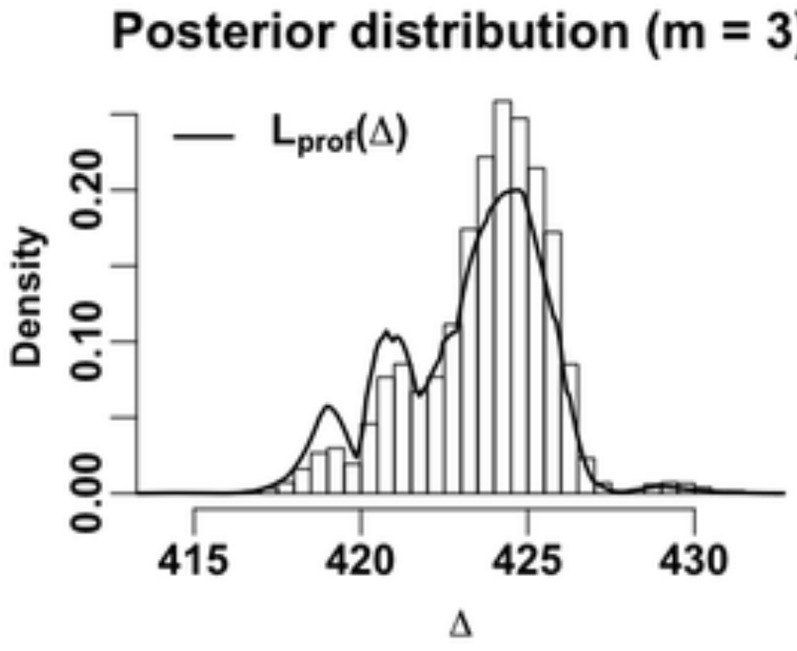

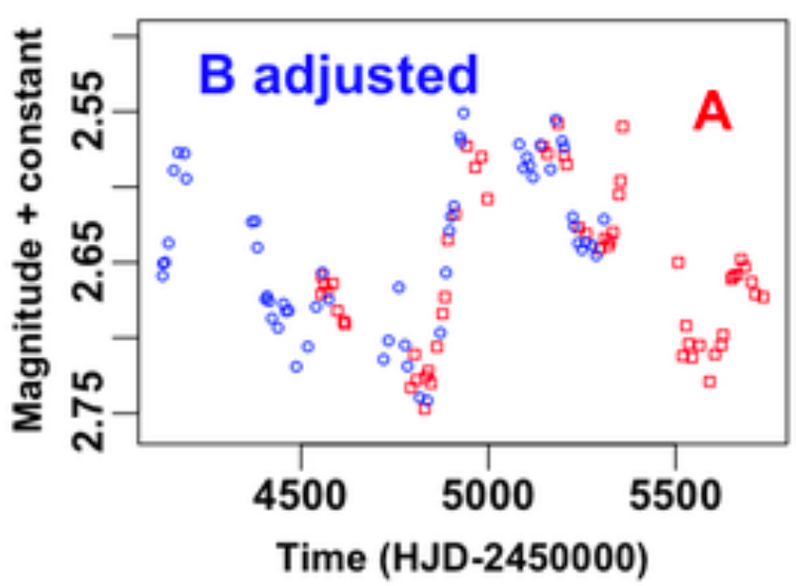

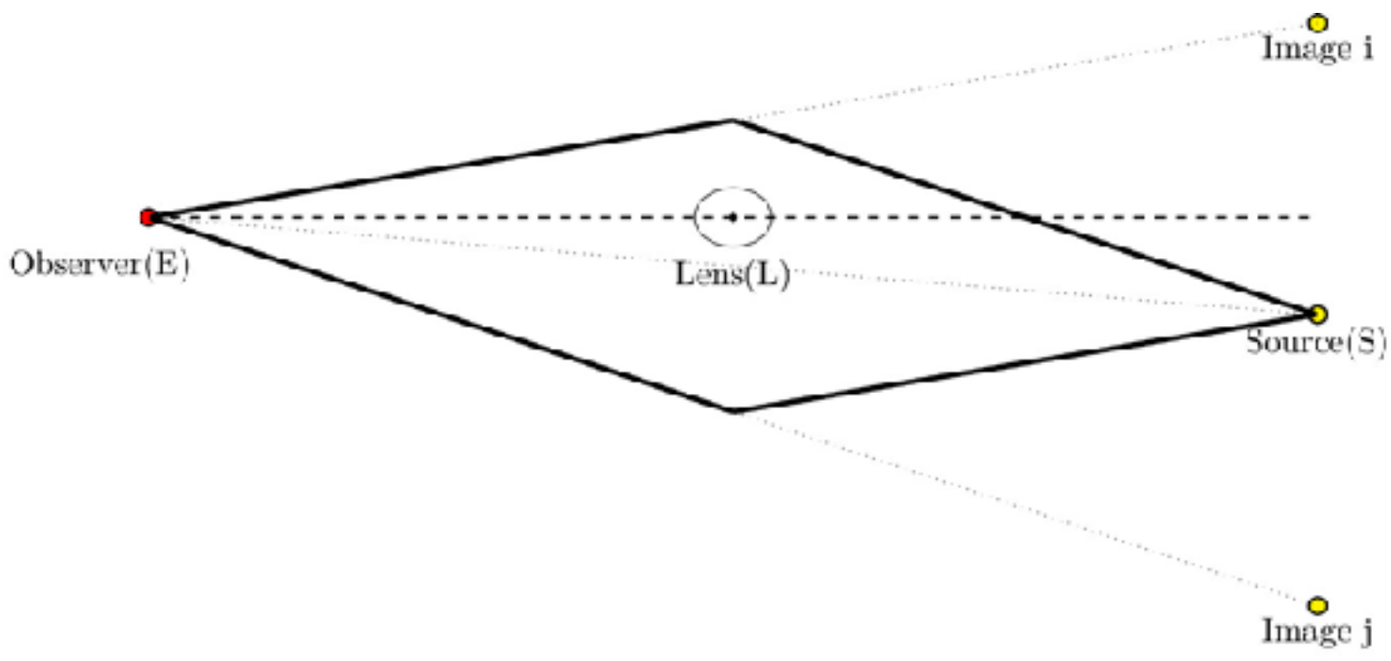

1985 ... discovery of *the Einstein Cross by J. Huchra*
a nearby galaxy with a peculiar spectrum ...

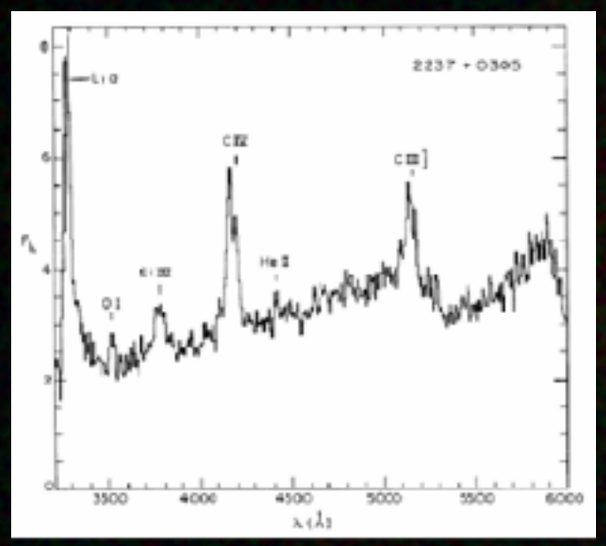

Einstein Cross seen with the Hubble Space Telescope

1987

... discovery of *Gravitational Arcs in massive clusters:*

Every cluster is a potential strong lens ...

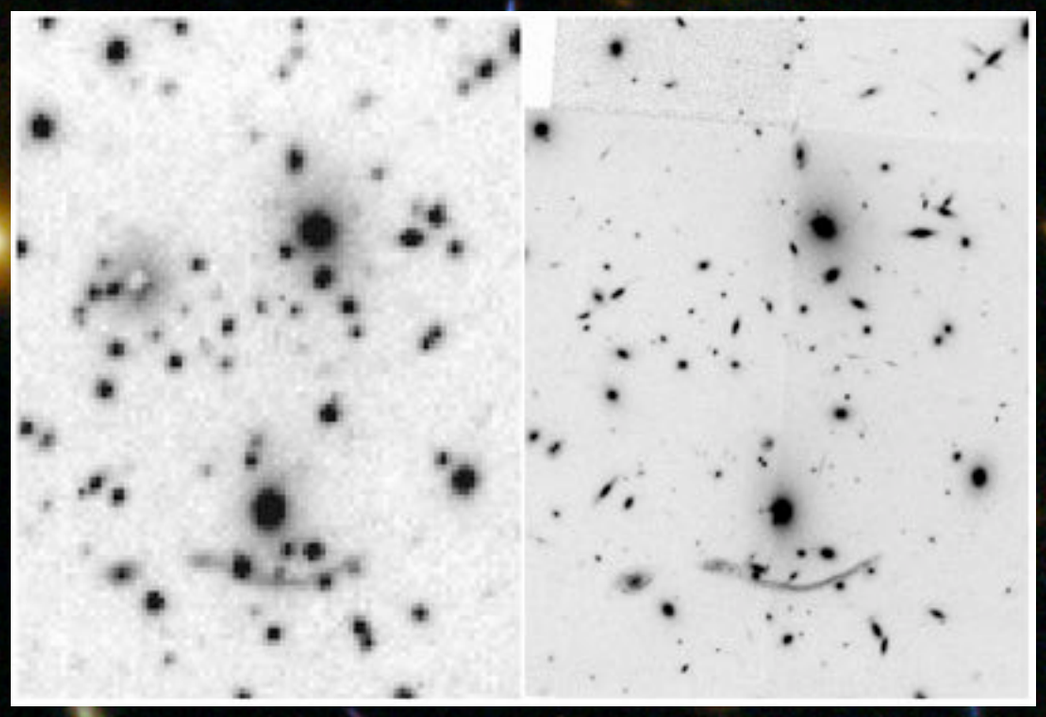

Giant Arc in A370 seen with the Hubble Space Telescope

2005

... searching through SDSS spectroscopic surveys: discoveries of many galaxy-lens systems

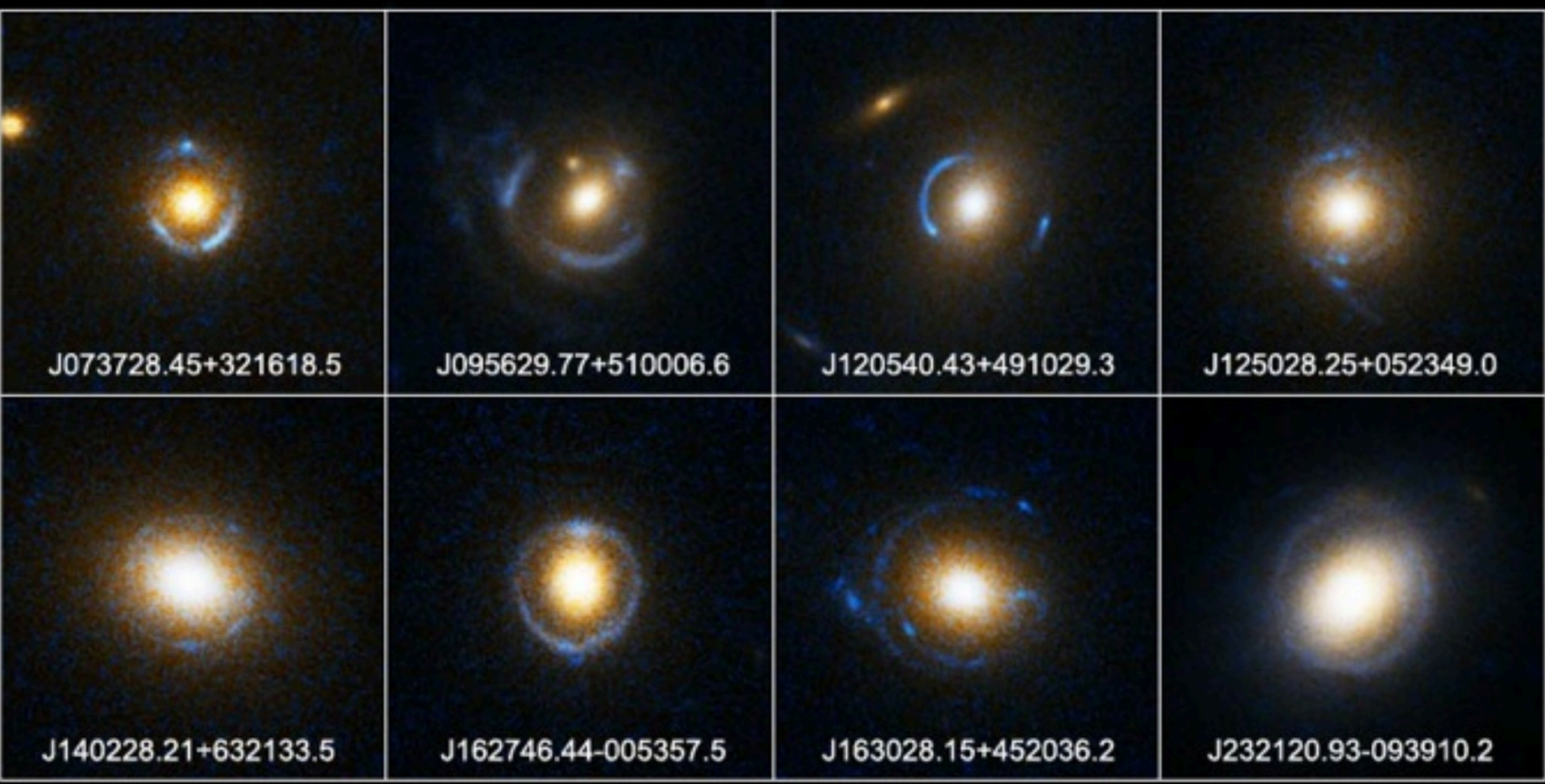

2007

... an almost perfect ring in the SDSS survey: weighting galaxy mass (stellar and dark) ...

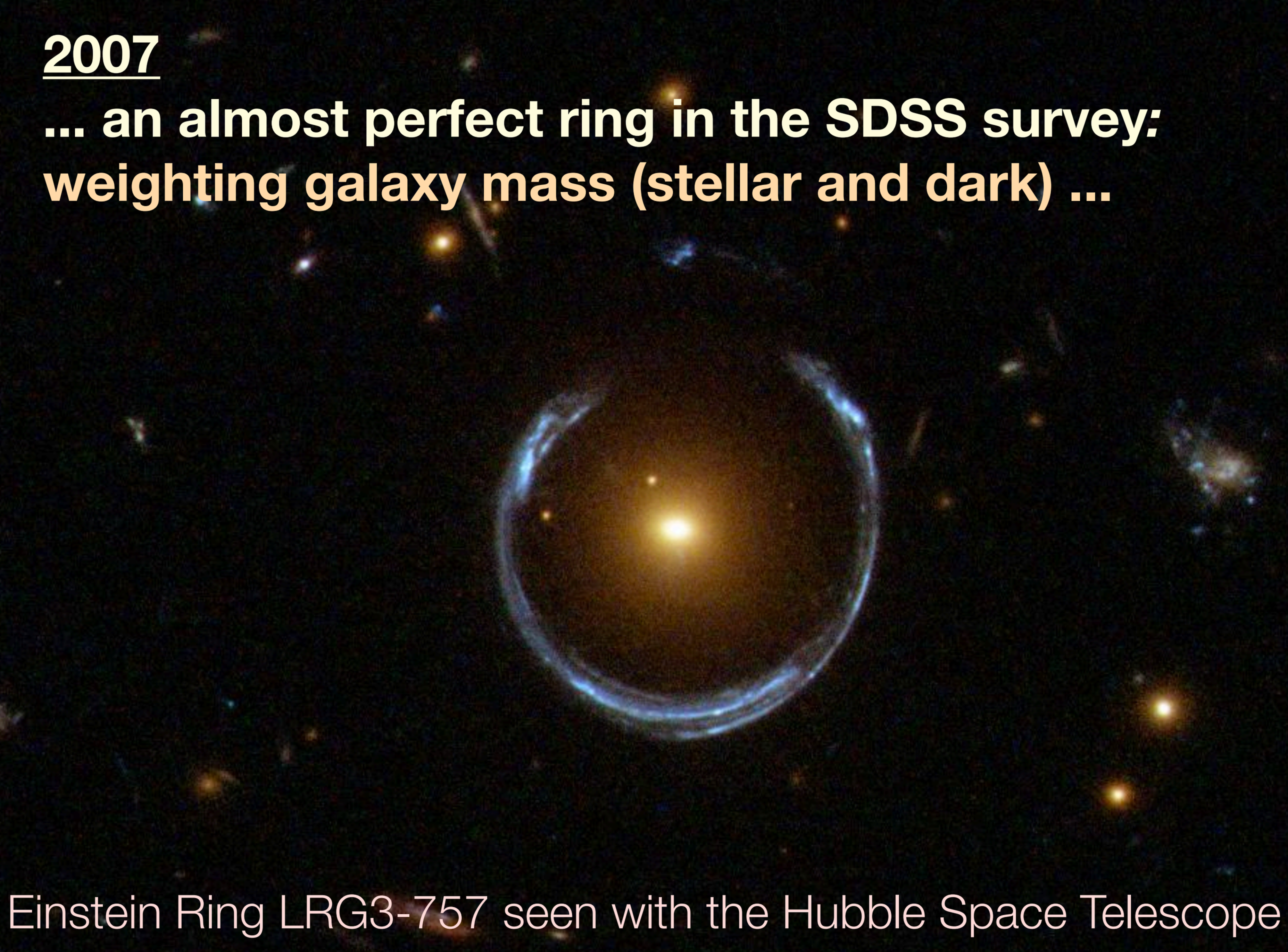

Einstein Ring LRG3-757 seen with the Hubble Space Telescope

RA,Dec = 177.1375, 19.5008, zoom 15

https://www.legacysurvey.org/viewer?ra=177.1375&dec=19.5008&layer=ls-dr9&zoom=15

- Images
  - Legacy Surveys DR9 images
  - Legacy Surveys DR9 models
  - Legacy Surveys DR9 residuals
  - Legacy Surveys DR9.1.1 COSMOS deep
  - + Legacy Surveys DR9-north images
  - + Legacy Surveys DR9-south images
  - + Older Legacy Surveys
  - + unWISE W1/W2 NEO6
  - + More surveys
- Overlays
  - + Boundaries
  - + Imaging catalogs
  - + Spectroscopy
  - + DESI
  - Bright Objects
    - Bright stars
    - Tycho-2 stars
    - Star clusters & Planetary Nebulae
    - NGC/IC galaxies
    - Siena Galaxy Atlas
    - HyperLEDA/SGA galaxies
    - DR9 Photo-z
    - Constellations

30 arcsec

Contrast: 1

Brightness: 1

Jump to object: NGC 5614

Custom catalog upload (FITS table; RA,Dec,[name]):
Choose file No file chosen Upload

2009: ~100 lenses in SLACS

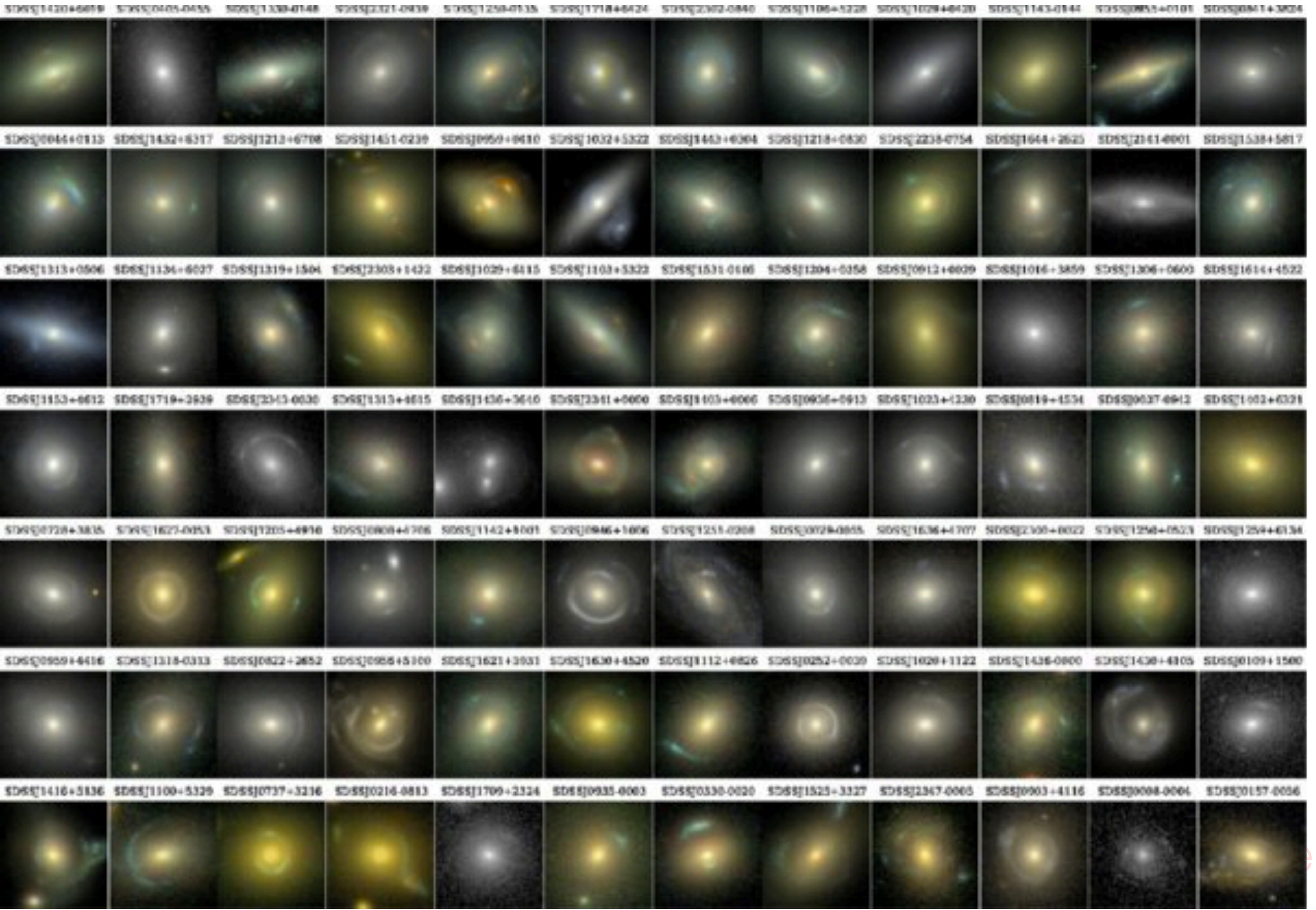

2012 : ~37 cluster lenses in SDSS follow-up images taken with HST

2014 : Hubble Frontier Fields Observation of 6 massive clusters (MACSJ0717)

2015 : Refsdal Supernovae in Frontier Field MACSJ1149

April 6, 2018: Hubble Finds an Einstein Ring

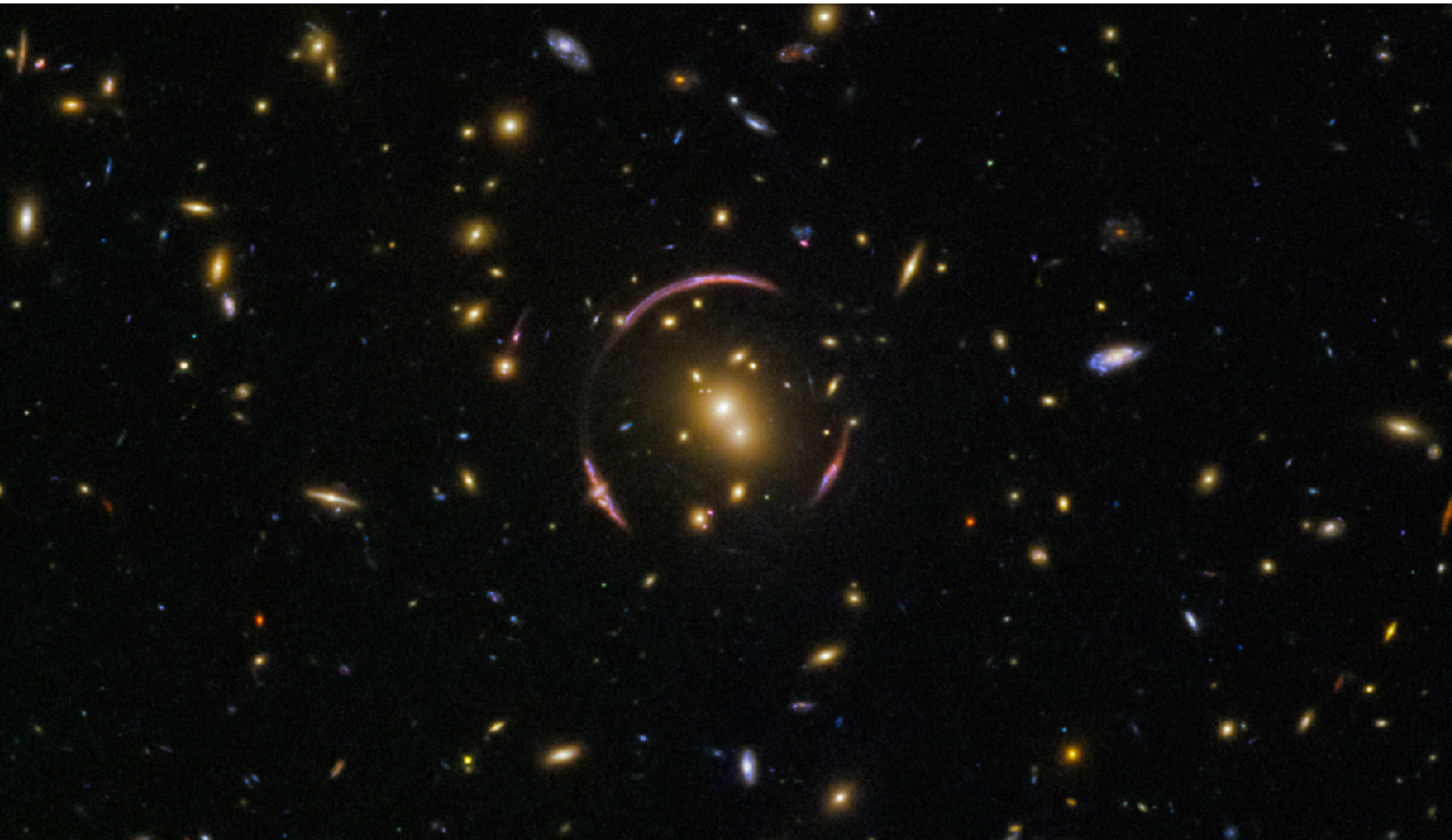

Extreme magnification of an individual star at redshift 1.5 by a galaxy-cluster lens

Kelly et al 2018, Nature Astronomy - April 2nd, 2018

Hubble Frontier Field Cluster MACS J1149

Observations: Follow-up of the SN Refsdal

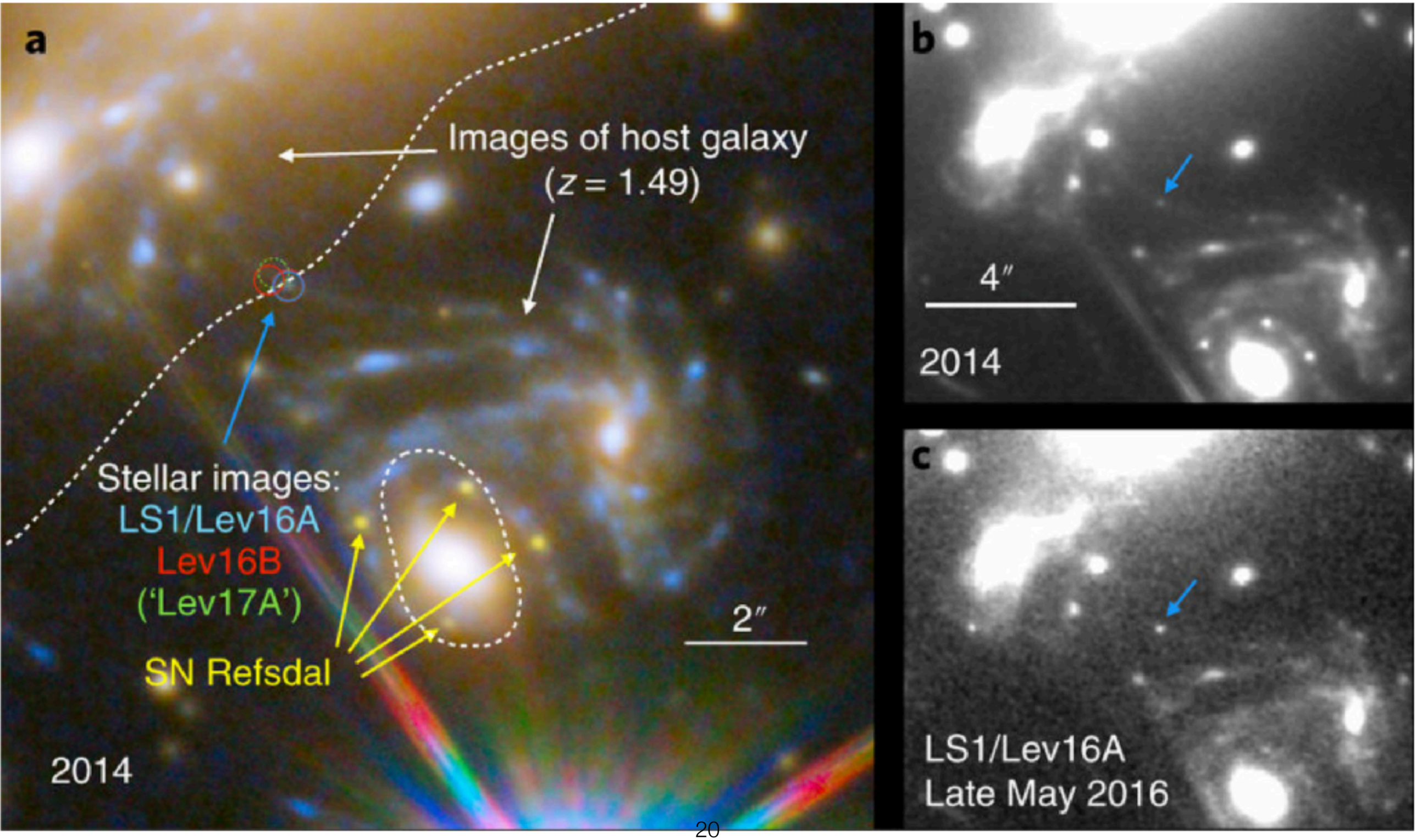

Hubble Frontier Field Cluster MACS J1149

Cluster Lens Modeling Uncertainties

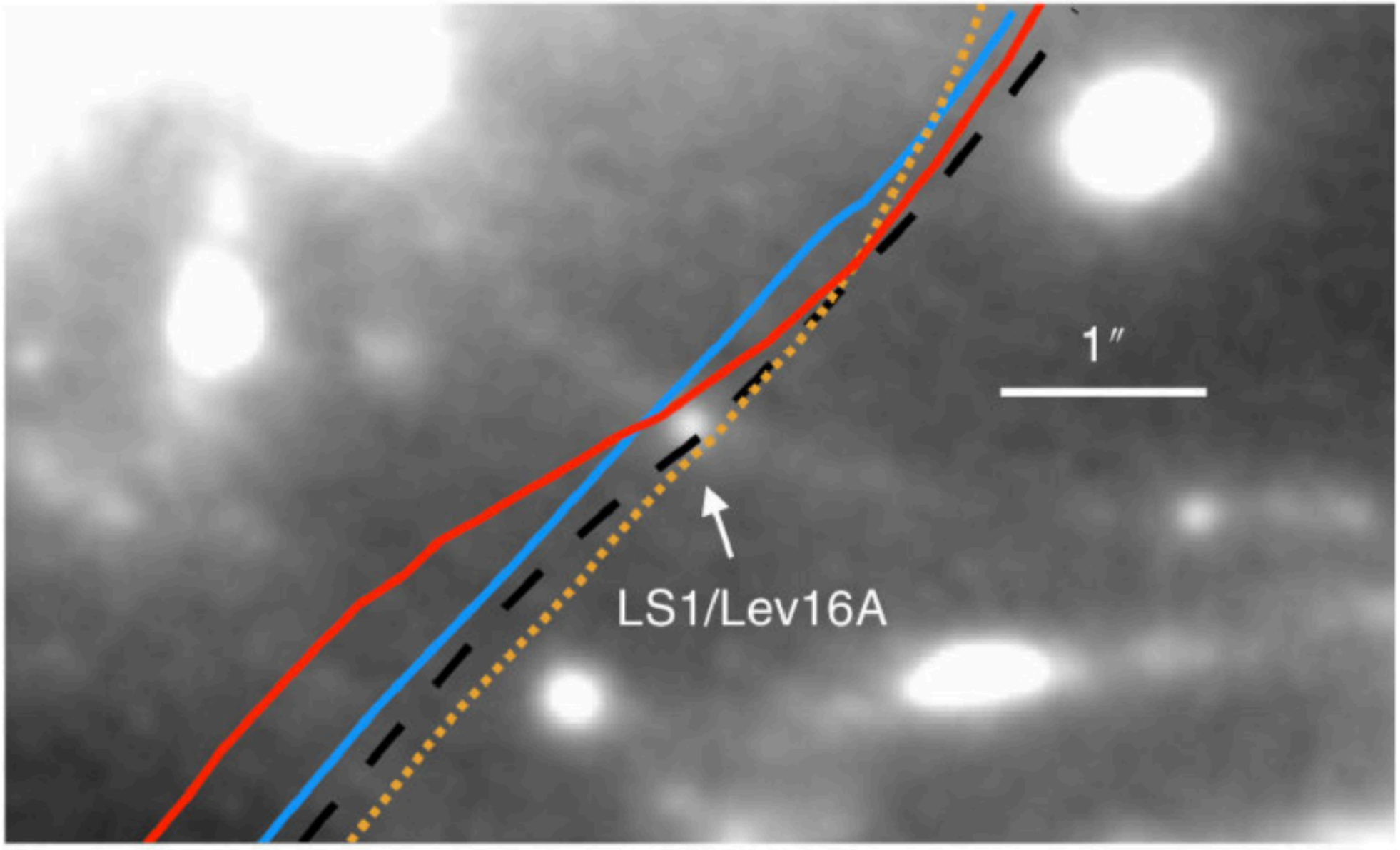

Critical curves for models with available high-resolution lens maps including ref. [8] (CATS; solid red line), ref. [40] (dotted orange line), ref. [10] (solid blue line) and ref. [76] (dashed black line) are superposed on the HST WFC3 IR F125W image. Although predictions for the location of the critical curve near LS1 disagree by ~0.25″, LS1 lies within ~0.13″ of all of these models' predictions.

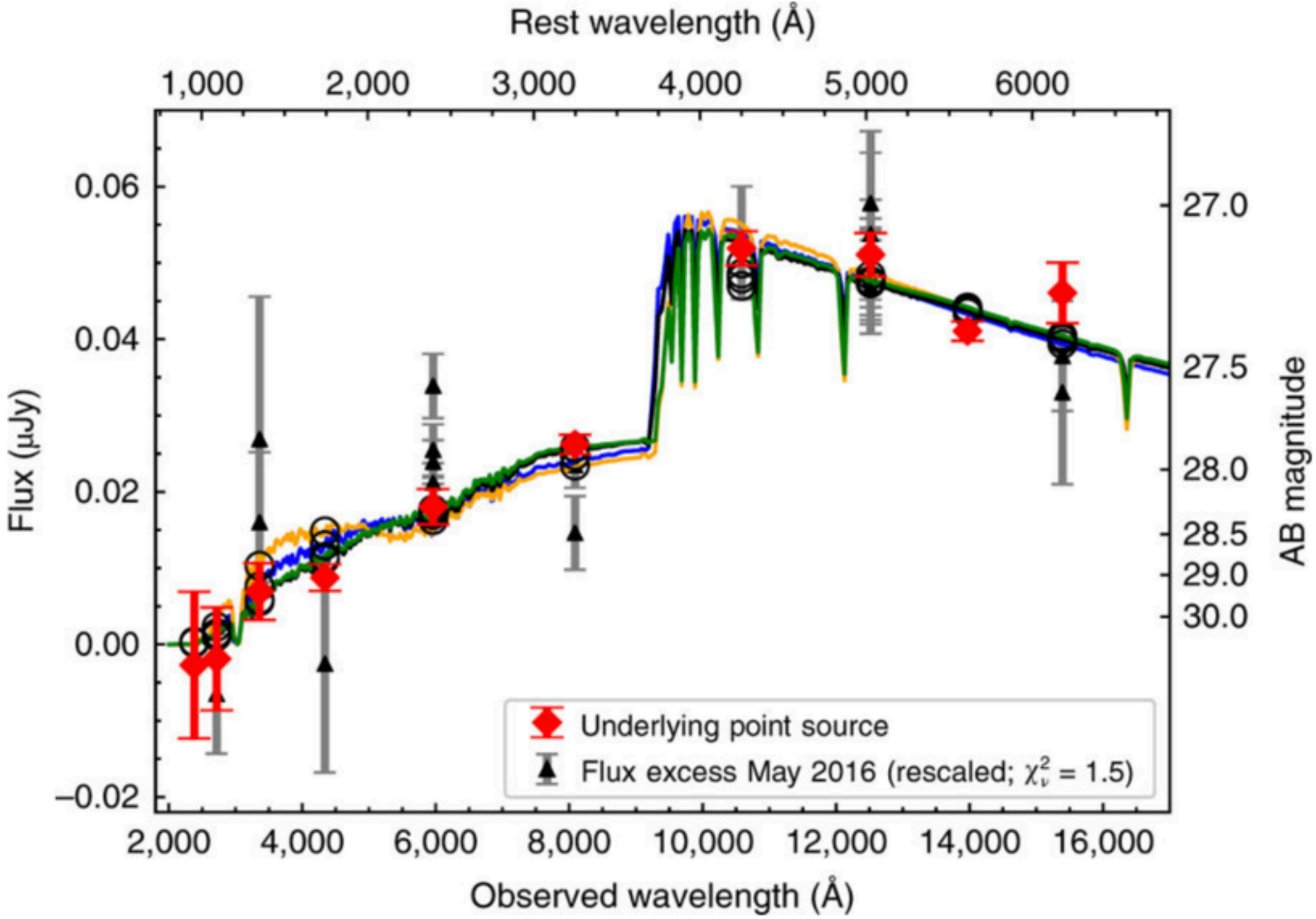

Rescaling the SED of the flux excess (Lev16A; black triangles) to match that of the 2013–2015 source (red diamonds) yields $\chi^2_\nu = 1.5$, indicating that they are statistically consistent with each other despite a flux density difference of a factor of ~4. The SED shows a strong Balmer break consistent with the host-galaxy redshift of 1.49, and stellar atmosphere models[17] of a mid-to-late B-type star provide a reasonable fit. Error bars correspond to 68% confidence intervals. The blue curve has T = 11,180 K, surface gravity $\log g = 2$, $A_V = 0.02$ and $\chi^2 = 16.3$; the orange curve has T = 12,250 K, $\log g = 4$, $A_V = 0.08$ and $\chi^2 = 30.6$; the black curve has T = 12,375 K, $\log g = 2$, $A_V = 0.08$ and $\chi^2 = 12.9$; and the green curve has T = 13,591 K, $\log g = 4$, $A_V = 0.13$ and $\chi^2 = 16.5$. Black circles show the expected flux density for each model. Error bars correspond to 68% confidence levels.

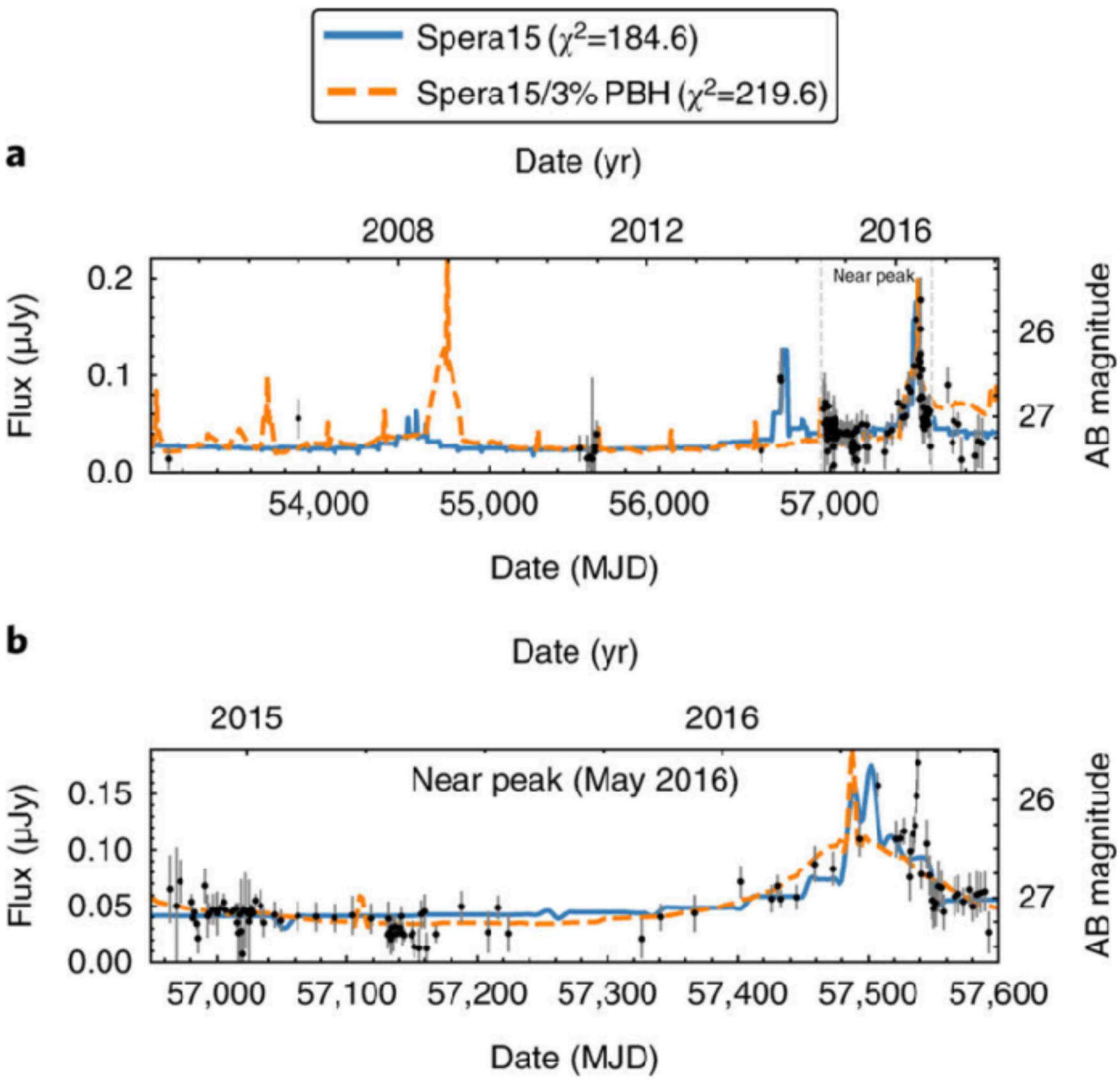

Black circles show fluxes measured through all wideband HST filters converted to F125W using LS1's SED. Error bars correspond to 68% confidence levels. **a**, LS1's full HST light curve, which begins in 2004. **b**, The most densely sampled part of the light curve including the May 2016 peak (Lev16A). This maximum shows two successive peaks that may correspond to a lensed binary system of stars at $z = 1.49$. MJD is modified Julian date. Error bars correspond to 68% confidence levels.

Ingredients for modeling

- Light curve measurement from the Hubble data
- Light curve simulation:
  - Background Galaxy: Transverse velocity of stars 200-2000 km/s, IMF of stars in the distant galaxies (more luminous stars are more likely to be lensed)
  - Mass model: smooth [marco-lensing] and compact [micro-lensing] components:DM (Compact DM? =>BHs)+galaxies (stars=> IMF)

Multiple image? More detections

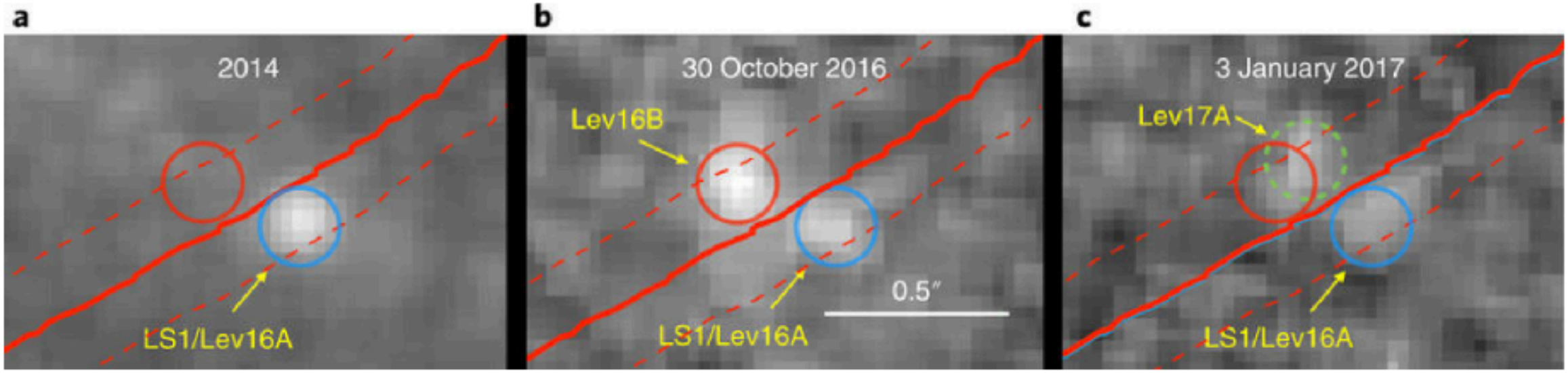

a, LS1 in 2014; we detected LS1 when it temporarily brightened by a factor of ~4 in late April 2016, and its position is marked by a blue circle. **b**, The appearance of a new image dubbed Lev16B on 30 October 2016, whose position is marked by a red circle. The solid red line marks the location of the cluster's critical curve from the CATS cluster model[8], and the dashed red lines show the approximate 1σ uncertainty from comparison of multiple cluster lens models[5,6,7,8,9,10]. Lev16B's position is consistent with the possibility that it is a counterimage of LS1. **c**, The candidate named Lev17A at the location of the green dashed circle had a ~4σ significance detection on 3 January 2017. If a microlensing peak, Lev17A must correspond to a different star.

7 Nov 2019: The Sunburst Arc (12 images!)

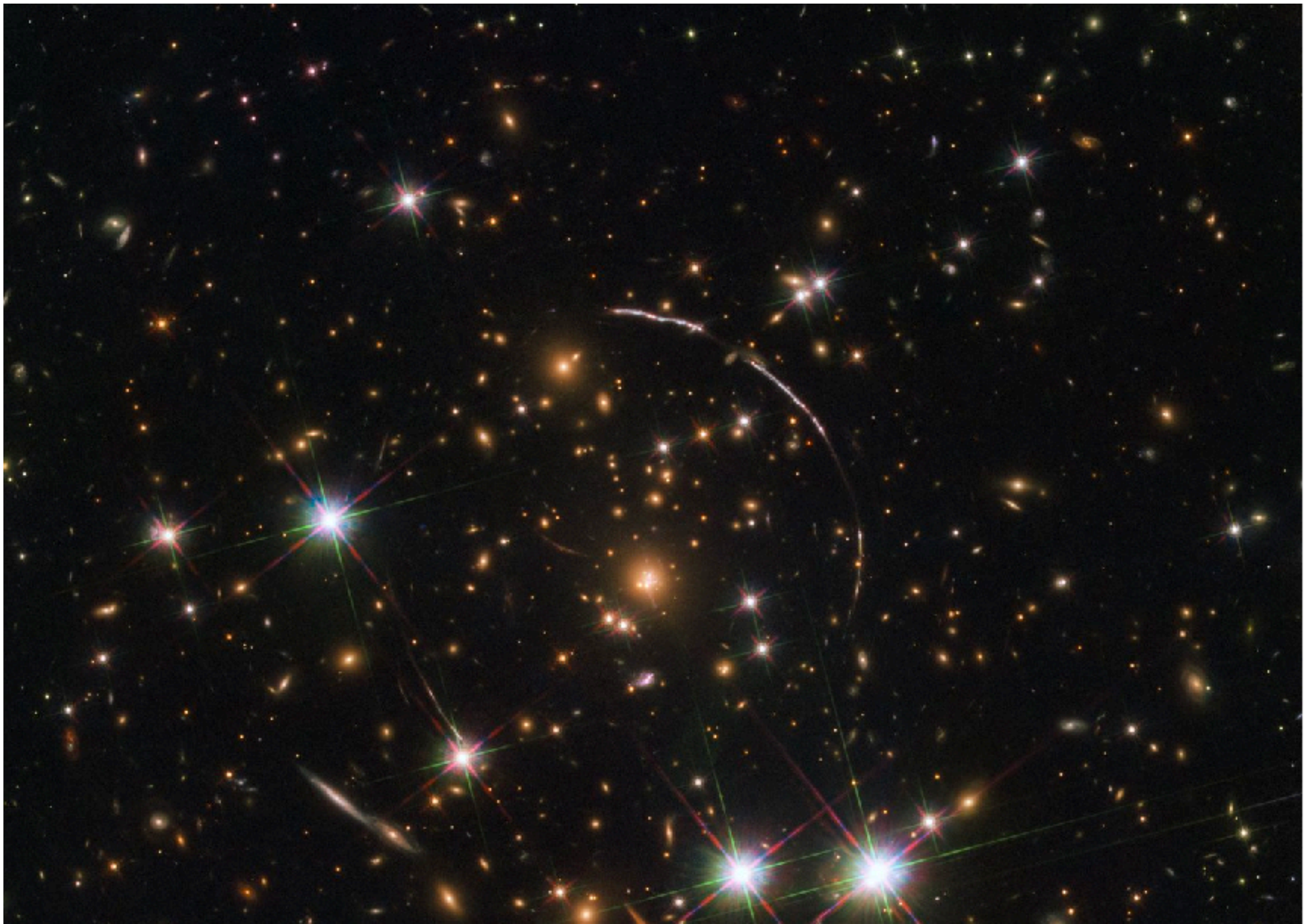

7 Nov 2019: The Sunburst Arc

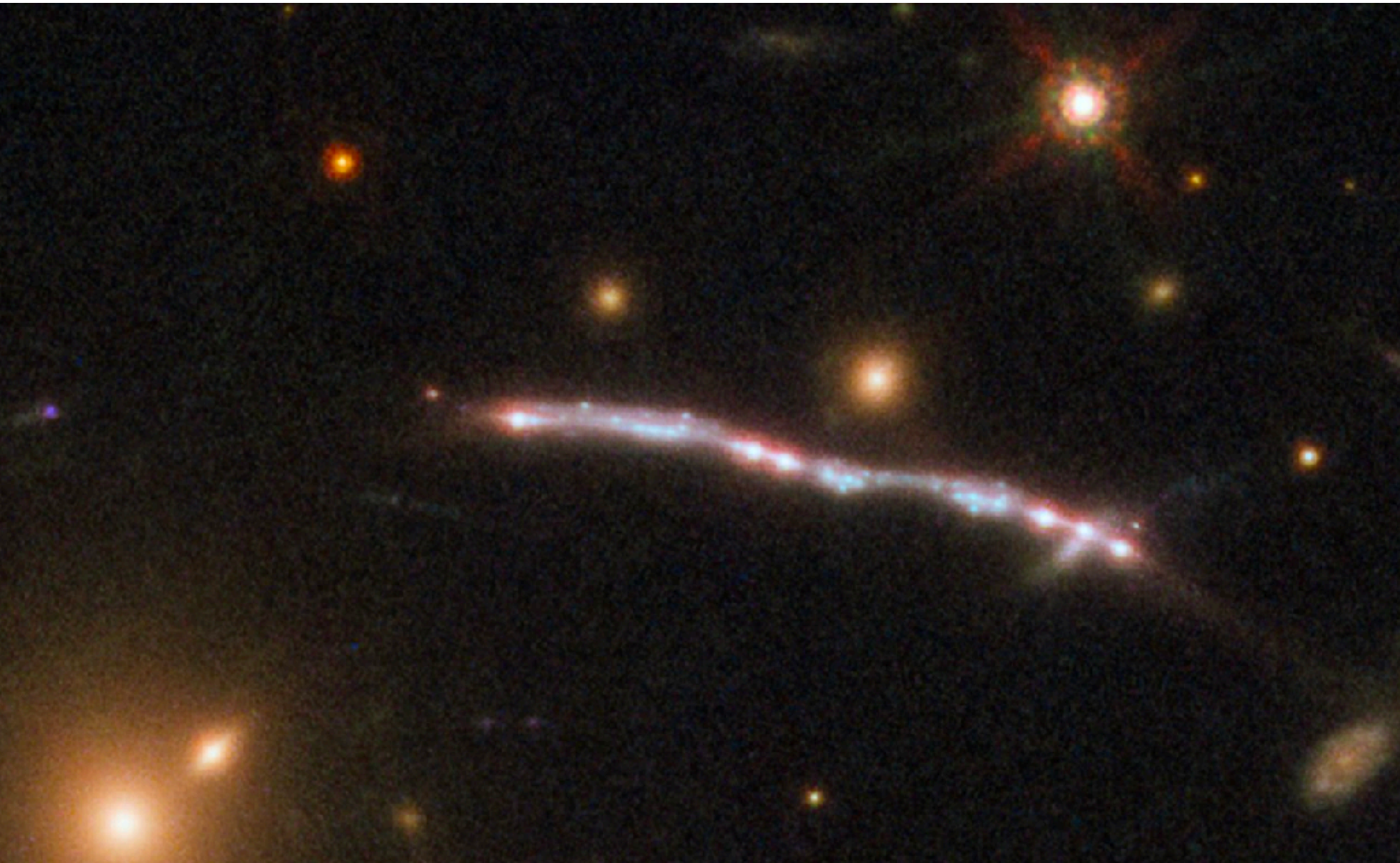

7 Nov 2019: The Sunburst Arc

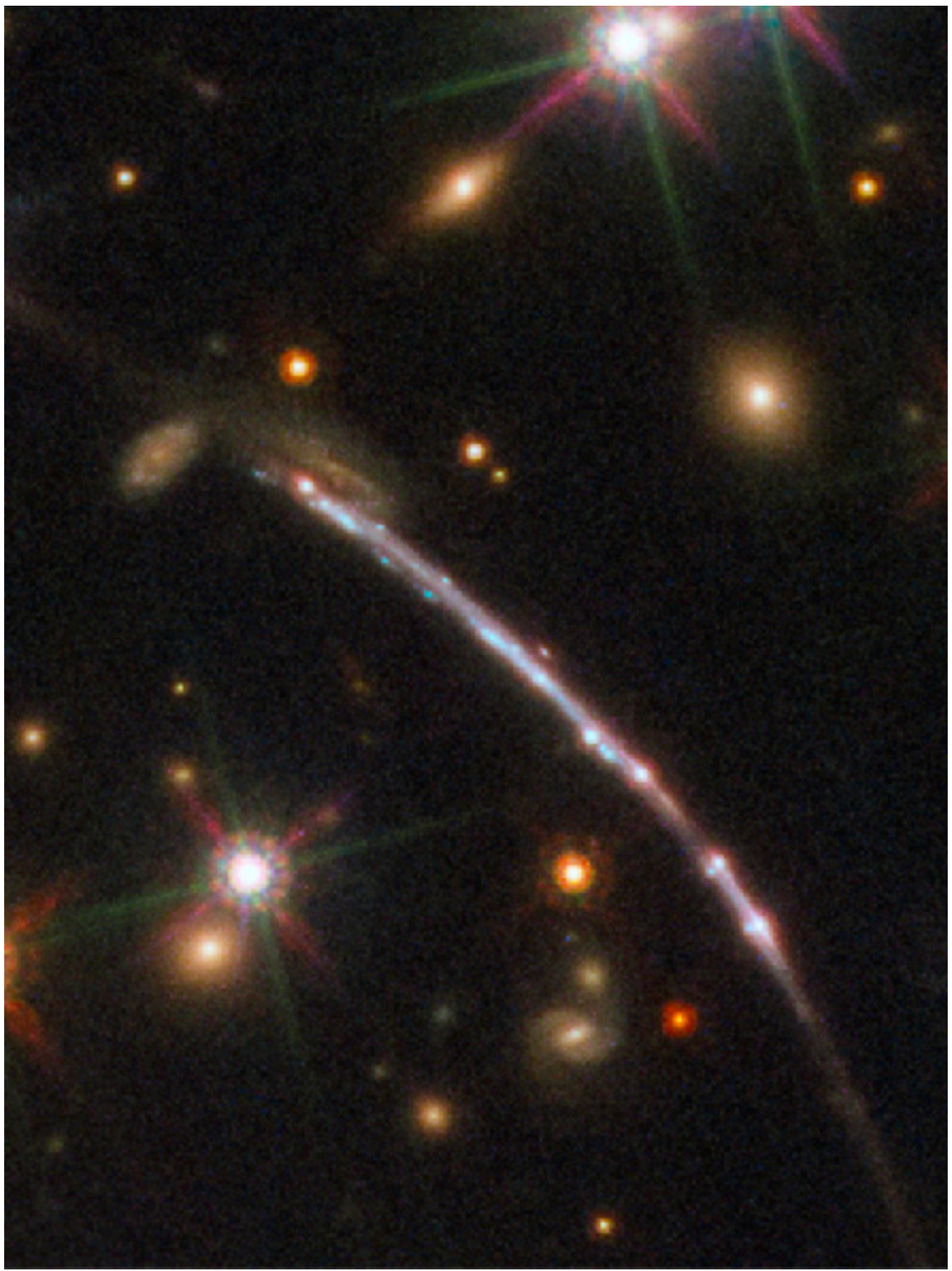

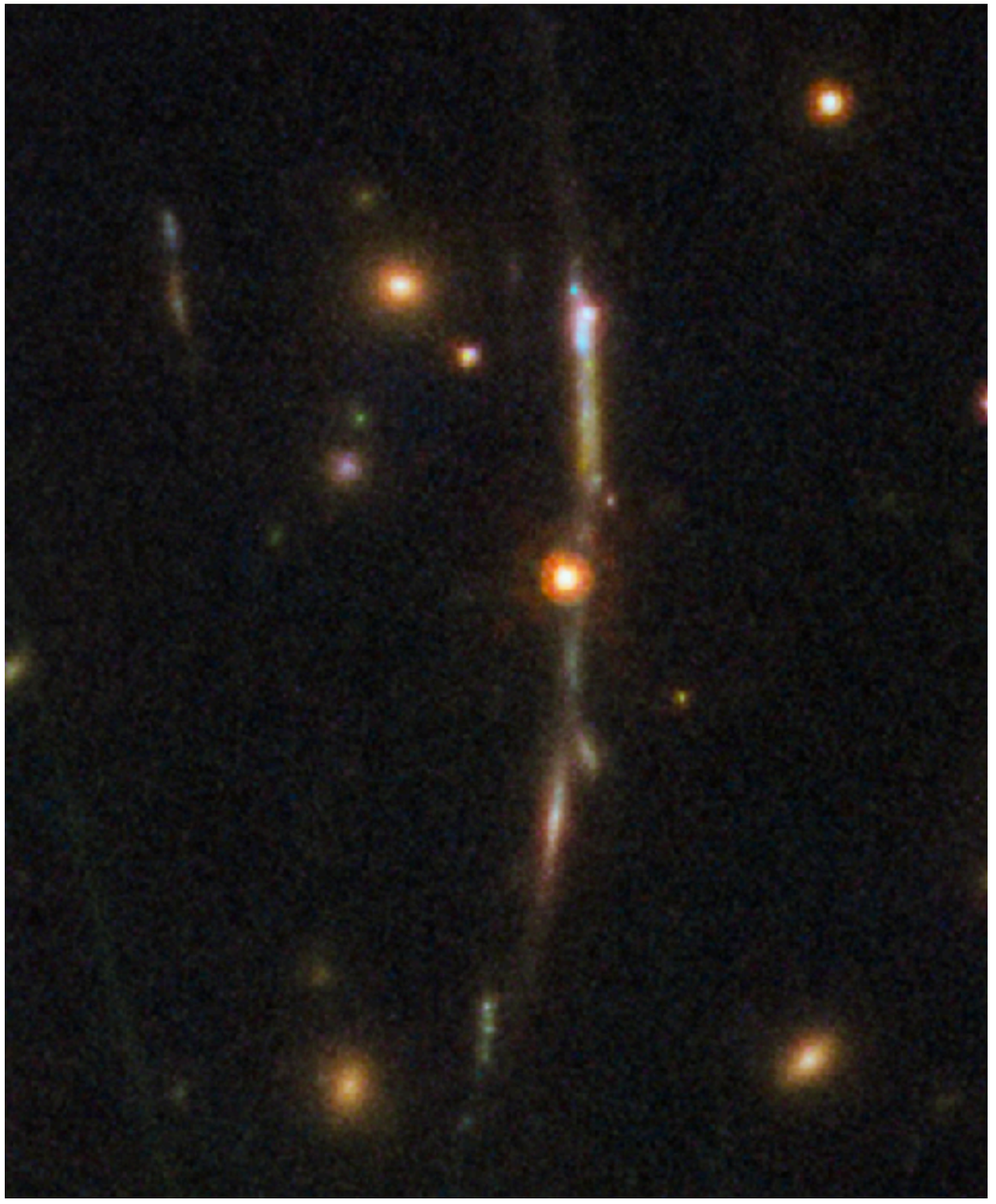

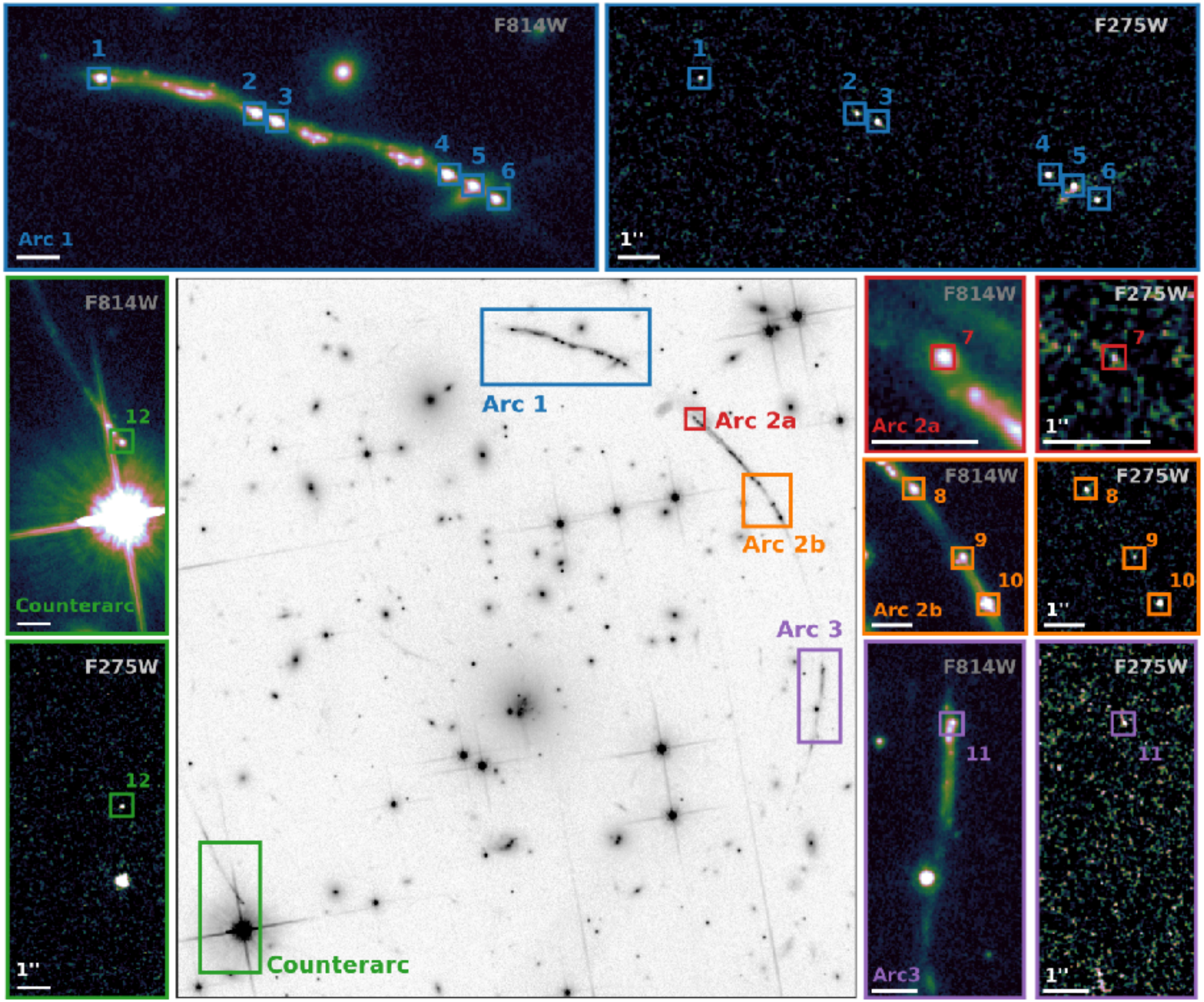
F814W
1
2
3
4
5
6
Arc 1
F275W
1''
12
Counterarc
Arc 1
Arc 2a
Arc 2b
Arc 3
Counterarc
7
8
9
10
11

July 2022: Galaxy Cluster SMACSJ0723 seen by JWST

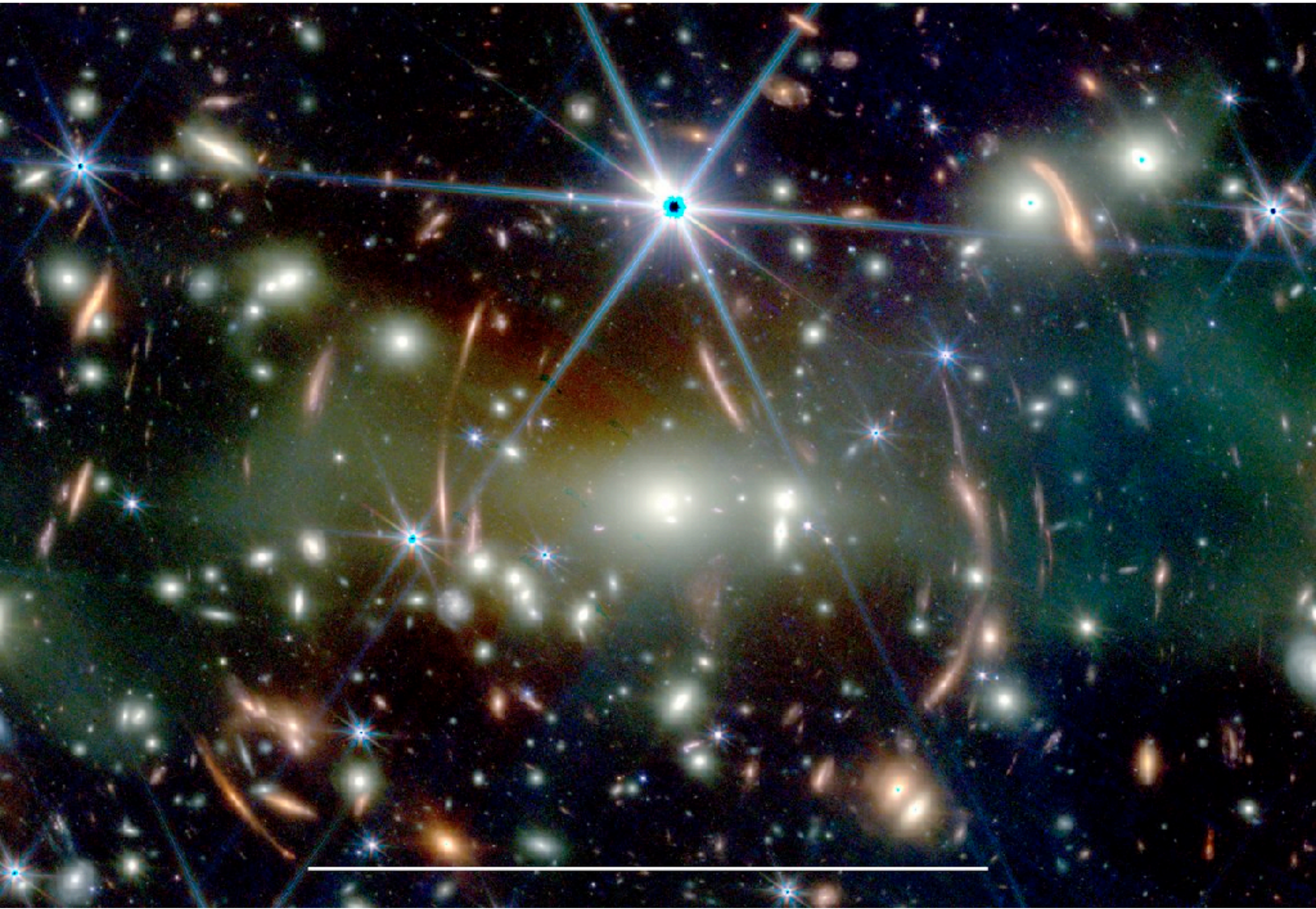

MACS J0138 Hubble and Webb Side-by-Side

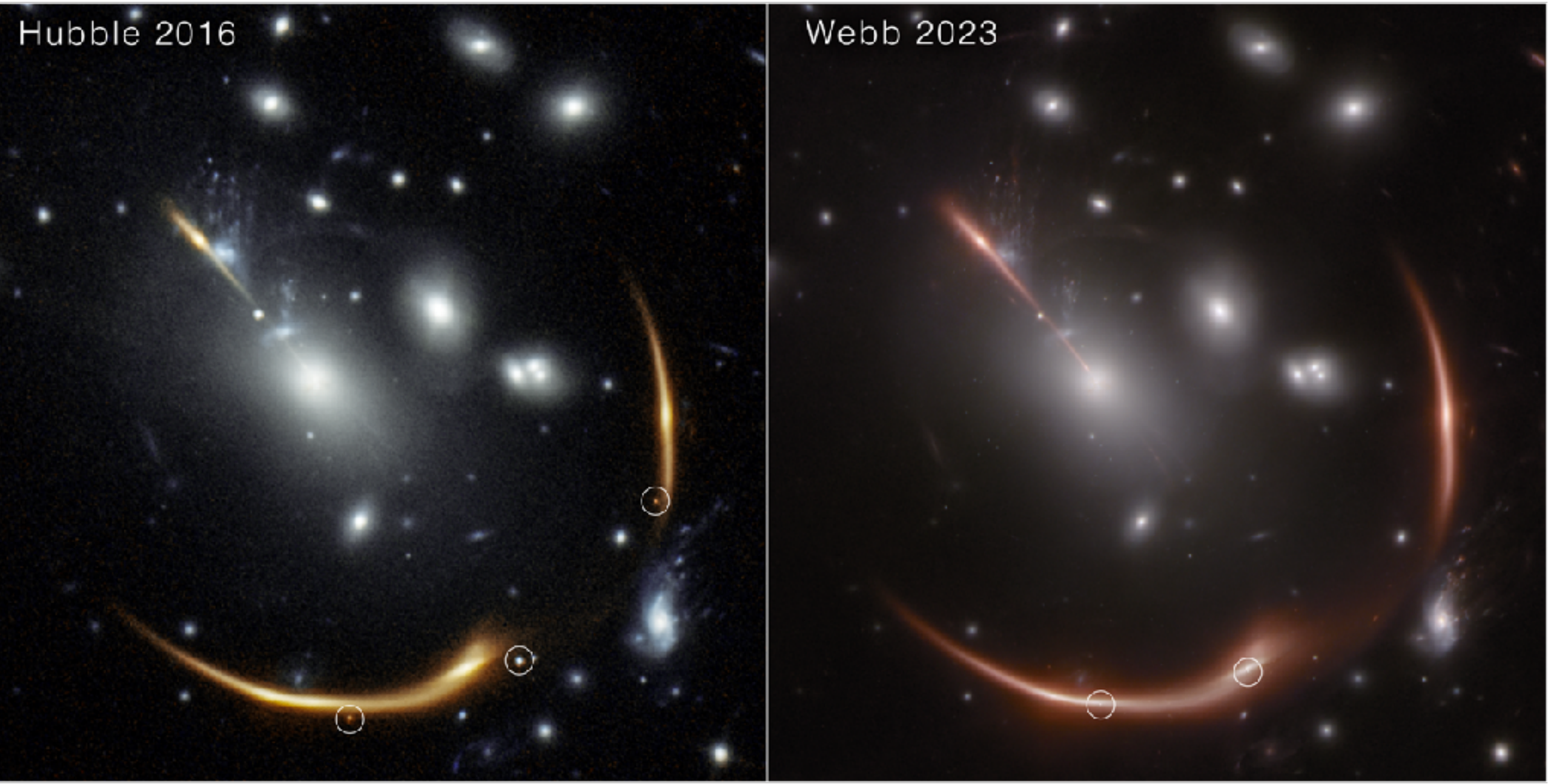

JAMES WEBB SPACE TELESCOPE

QUESTION MARK GALAXY | MACS J0417.5-1154

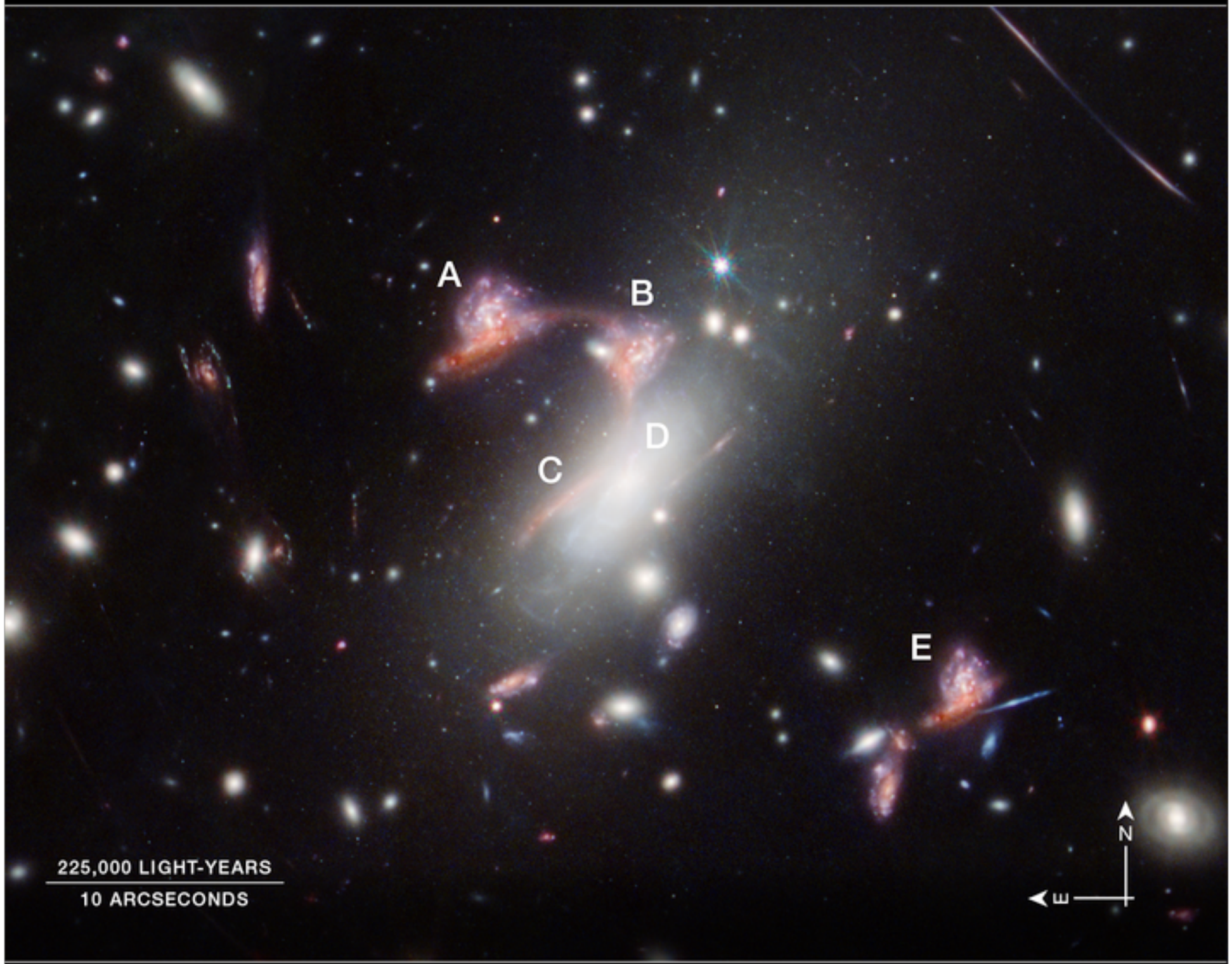

JWST NIRCam Filters | F090W F150W F444W

JAMES WEBB SPACE TELESCOPE

EL GORDO | ACT-CL J0102-4915

NIRCam Filters | F115W F150W F200W F277W F356M F444W

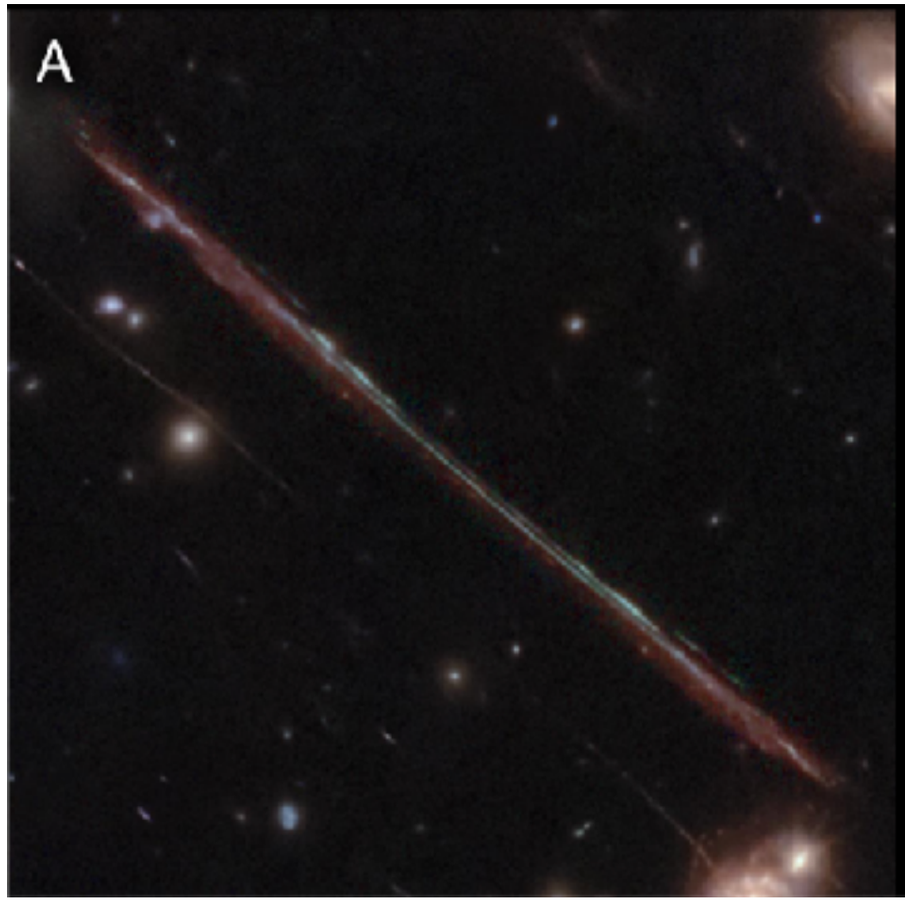

SDSS J1226+2149

Strong Lensing Basics

Cluster Lensing - Back to Basics

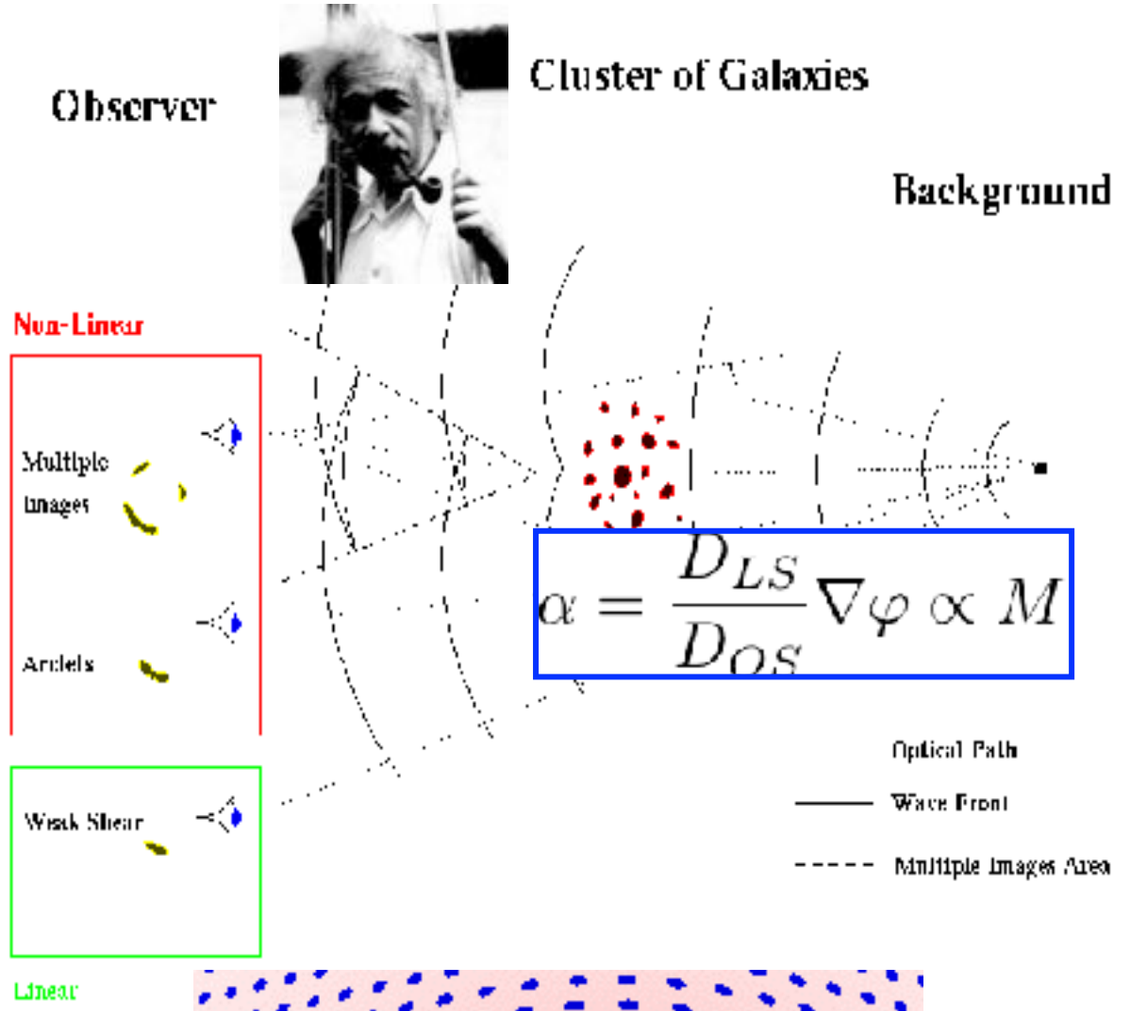

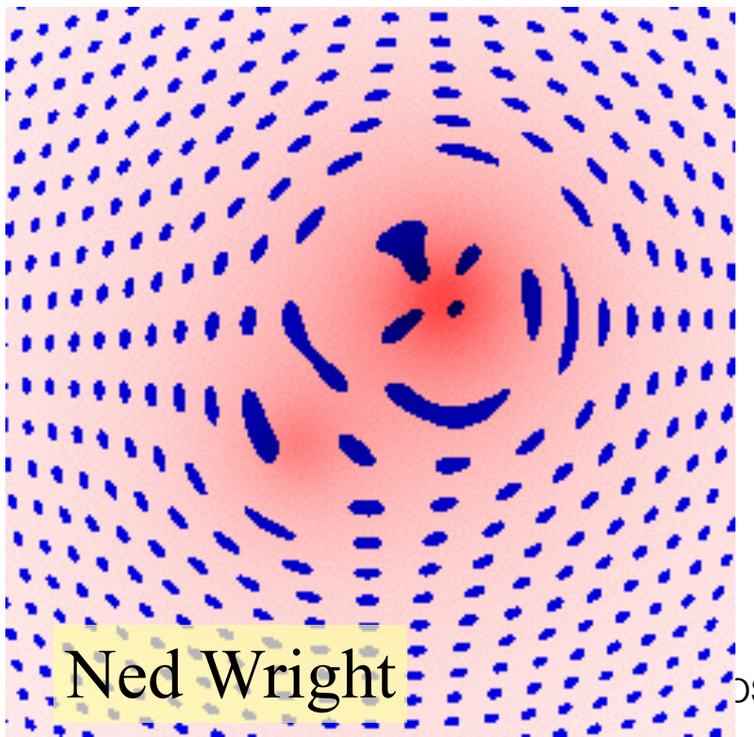

osmology

- **Basics of lensing:**
  - Large mass over-densities locally deform the Space-Time
  - *A pure geometrical effect, no dependence with photon energy - depends on TOTAL MASS*
- **Lensing by (massive) clusters**
  - Deflection of ~10-50 arcsec
  - *strongly lens many background sources => allow detailed mass reconstruction at different scales: cluster core, substructures, large scales*
  - *~1 SL cluster-lens per ~10 sq. deg: potentially ~2000 to study, Probably only ~200 identified today, nearly 20 with "a good" (SL) mass model*

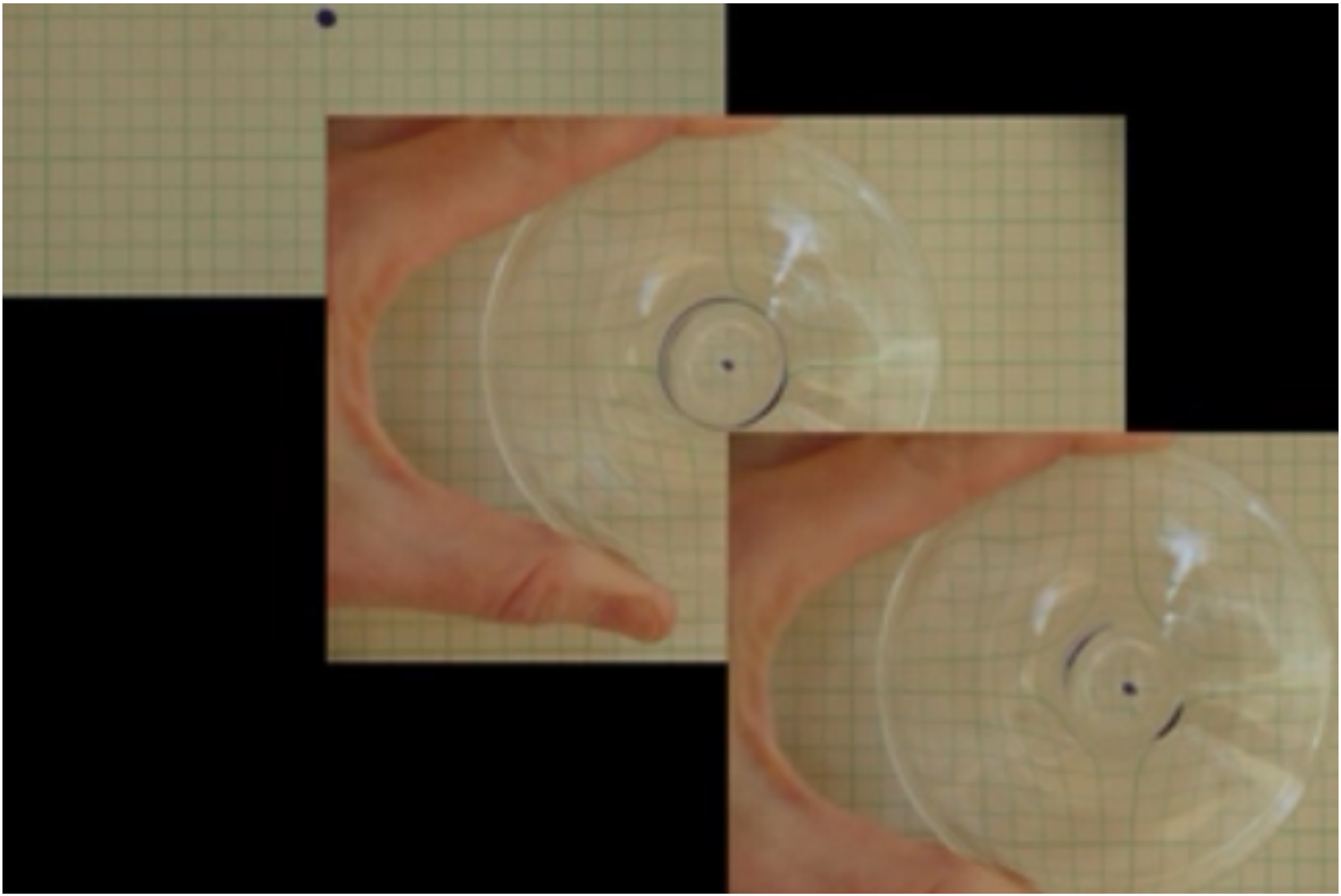

Gravitational lensing diagram

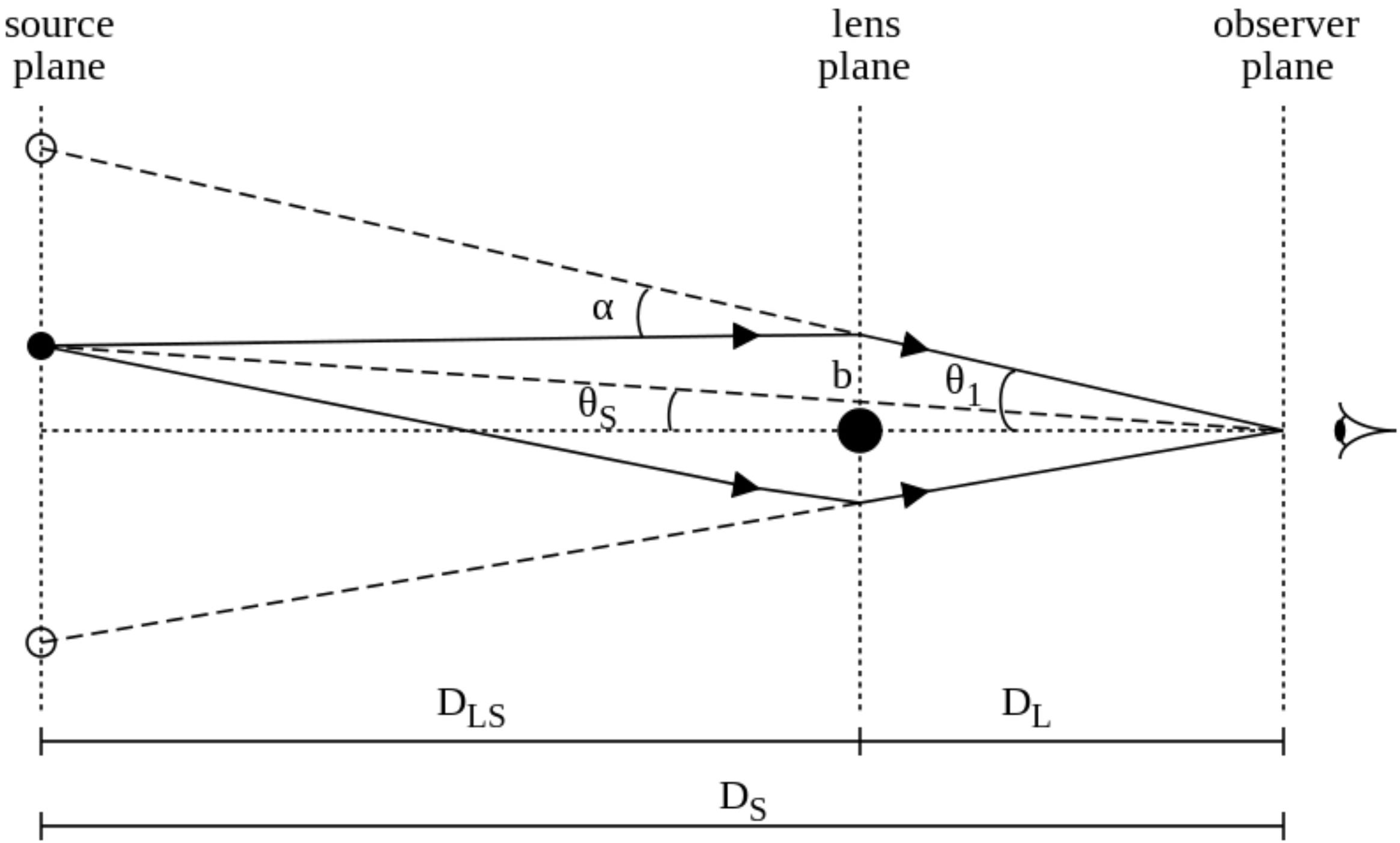

Lensing Equation

- Metric near a point mass

$$ds^2=(1+\frac{2\Phi}{c^2})c^2dt^2-(1-\frac{2\Phi}{c^2})dr^2$$

- Where Φ is the 3D gravitational potential

- Use the Fermat principle to find the effective light rays:

- $$\frac{dt}{d\theta_I}=0$$

Lensing Equations

Lens Mapping:

Lensing Potential

$$\vec{\theta}_S = \vec{\theta}_I - \frac{2\mathcal{D}}{c^2}\vec{\nabla}\phi_N^{2D}(\vec{\theta}_I) = \vec{\theta}_I - \vec{\nabla}\varphi(\vec{\theta}_I)$$

φ : lensing potential

$\Rightarrow$ Link with catastrophe theory

$\Rightarrow$ Parameters: Distances and Mass

$\Rightarrow$ Purely geometrical: *Achromatic effect*

Redshift and Cosmology

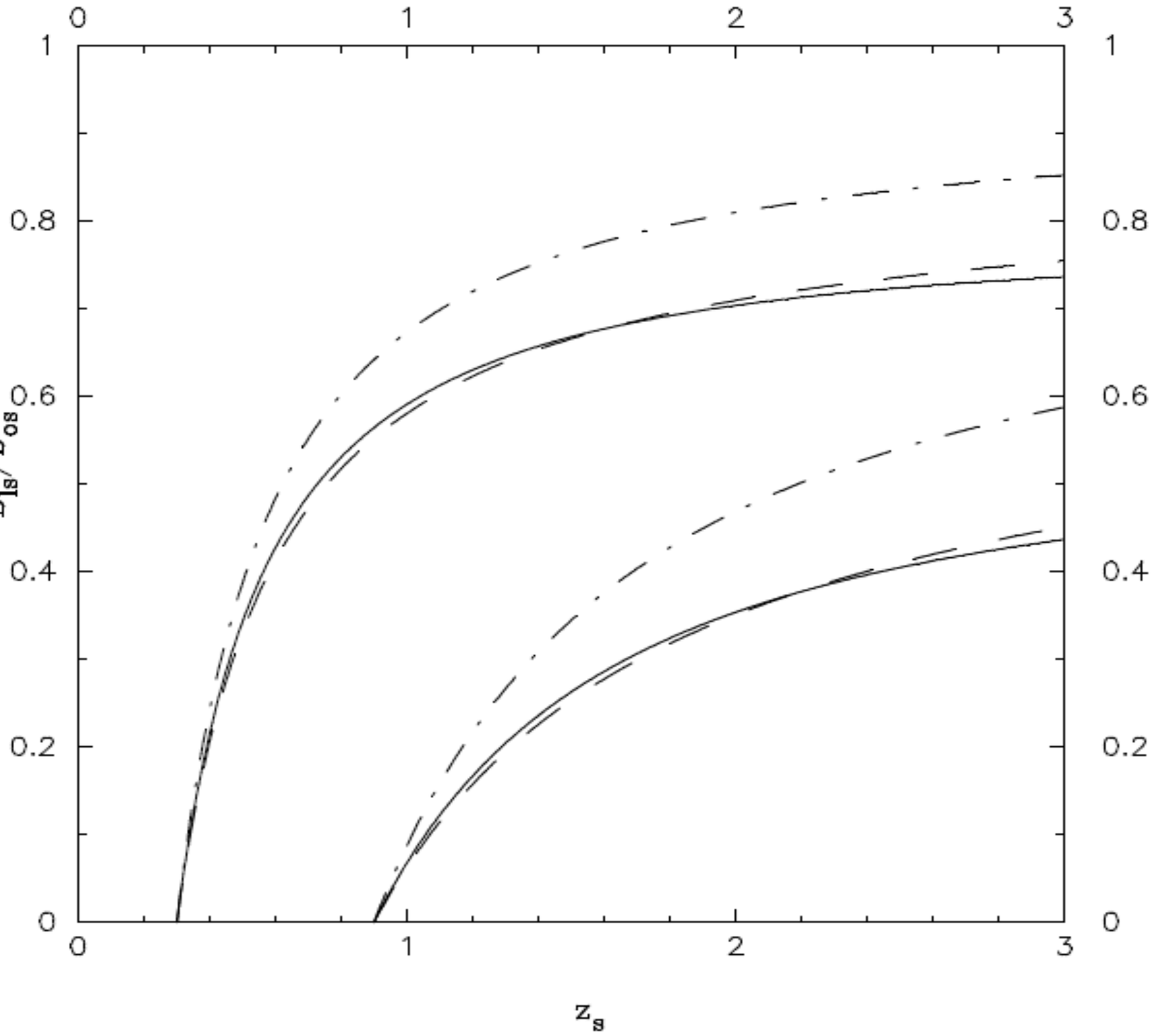

Lens Efficiency:

$$D_{LS}/D_{OS}$$

For a fixed lens redshift, the efficiency increase with source redshift

Weak cosmology dependence

Lensing Equations

Lens Mapping distortion (first order):

$$\frac{d\vec{\theta}_S}{d\vec{\theta}_I} = \mathcal{A}^{-1} = \begin{pmatrix} 1-\partial_{xx}\varphi & -\partial_{xy}\varphi \\ -\partial_{xy}\varphi & 1-\partial_{yy}\varphi \end{pmatrix}$$

In polar coordinates:

$$= \begin{pmatrix} 1-\partial_{rr}\varphi & -\partial_r\left(\frac{1}{r}\partial_\theta\varphi\right) \\ -\partial_r\left(\frac{1}{r}\partial_\theta\varphi\right) & 1-\frac{1}{r}\partial_r\varphi-\frac{1}{r^2}\partial_{\theta\theta}\varphi \end{pmatrix}$$

Lensing Equations

Amplification Matrix:

$$\mathcal{A}^{-1} = \begin{pmatrix} 1-\kappa-\gamma_1 & -\gamma_2 \\ -\gamma_2 & 1-\kappa+\gamma_1 \end{pmatrix}$$

κ: convergence

$$\kappa = \Delta\varphi/2 = \Sigma/2\Sigma_{crit}$$

$$\Sigma_{\rm cr} = \frac{c^2}{4\pi G}\frac{D_{\rm s}}{D_{\rm d}D_{\rm ds}} = 0.35\,{\rm g\,cm^{-2}}\left(\frac{D}{1\,{\rm Gpc}}\right)^{-1}$$

γ(γ_1,γ_2): shear vector

$$\gamma_1 = (\partial_{yy}\varphi - \partial_{xx}\varphi)/2 \qquad \gamma_2 = \partial_{xy}\varphi$$

Reduced shear:

$$g = \frac{\gamma}{1-\kappa}$$

Convergence and Shear

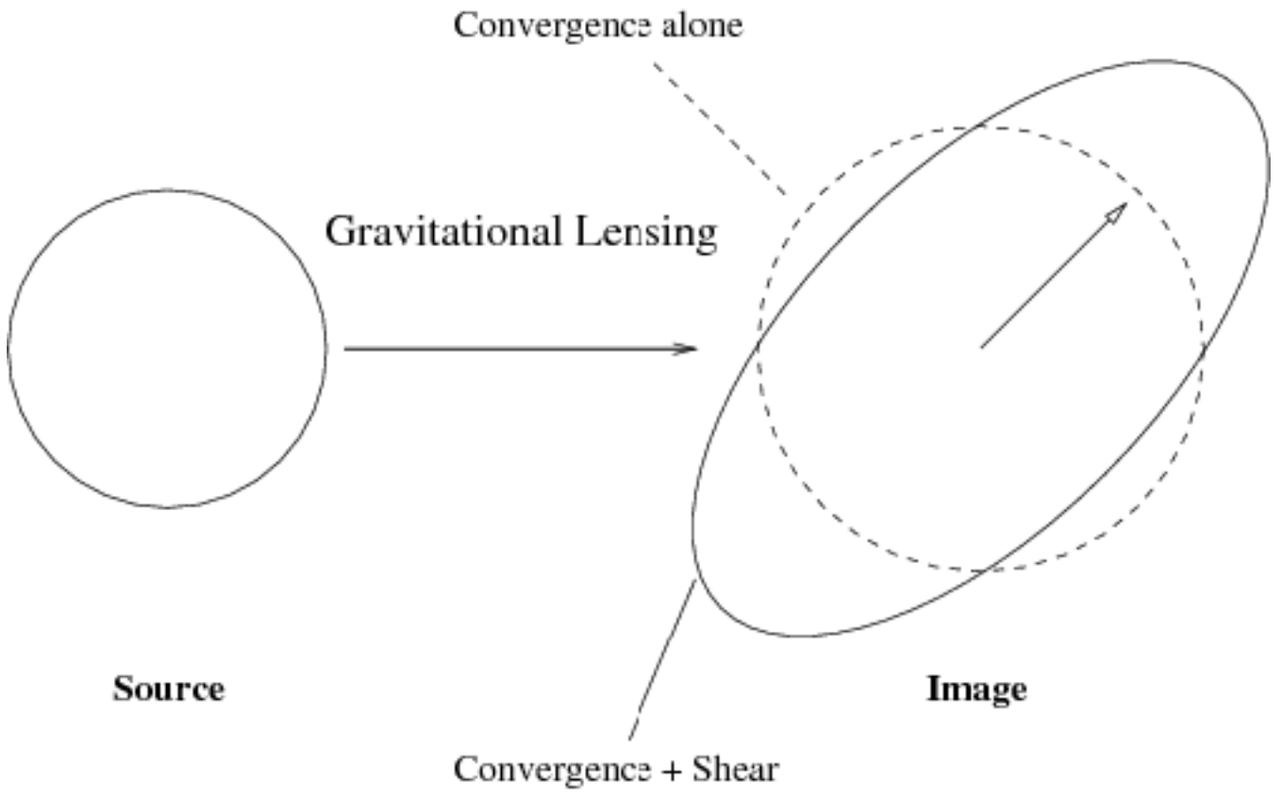

$$g = \frac{\gamma}{1-\kappa}$$

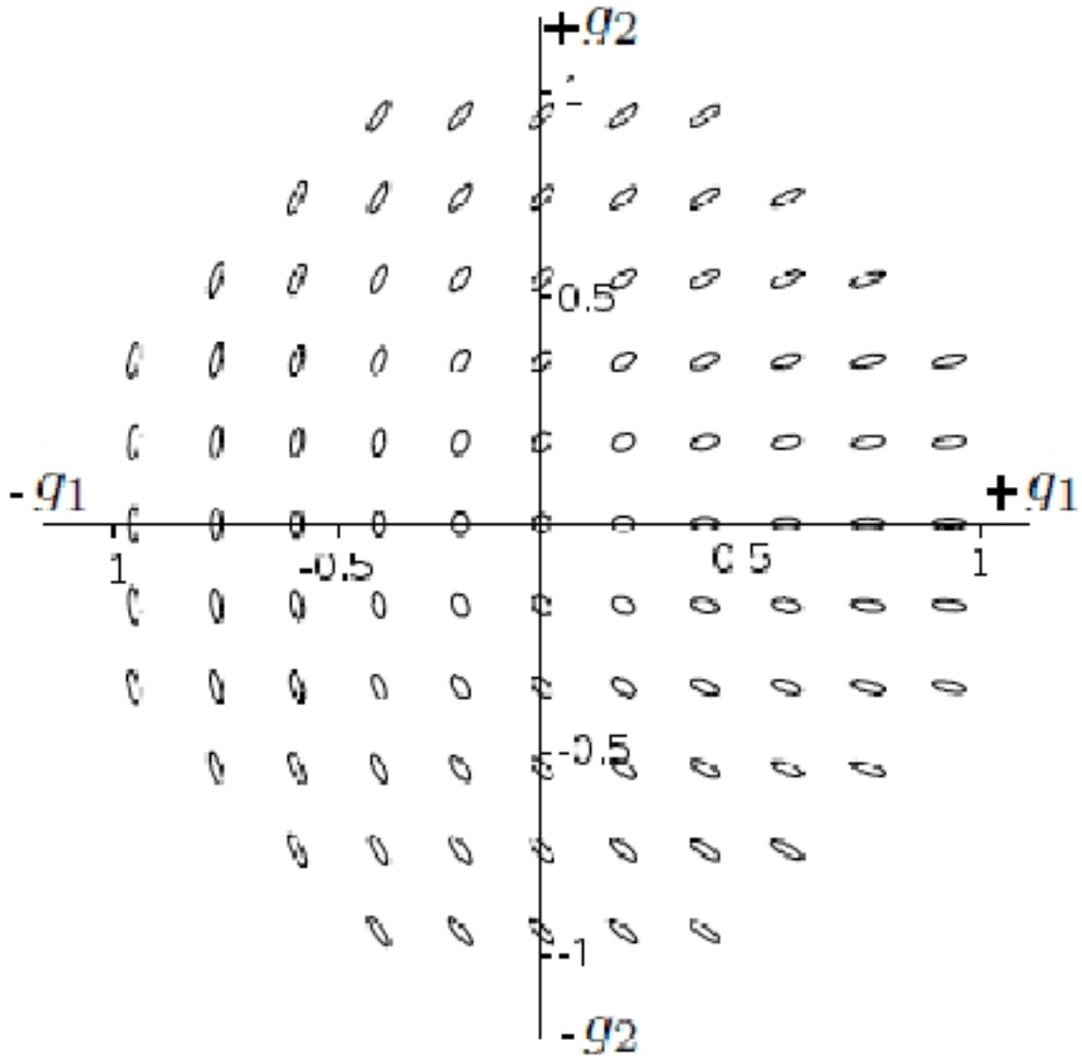

$$A^{-1} = \begin{pmatrix} 1-\kappa+\gamma & 0 \\ 0 & 1-\kappa-\gamma \end{pmatrix}$$

$$= (1-\kappa)\left[\begin{pmatrix} 1 & 0 \\ 0 & 1 \end{pmatrix} + \frac{\gamma}{1-\kappa}\begin{pmatrix} 1 & 0 \\ 0 & -1 \end{pmatrix}\right]$$

Convergence and Shear

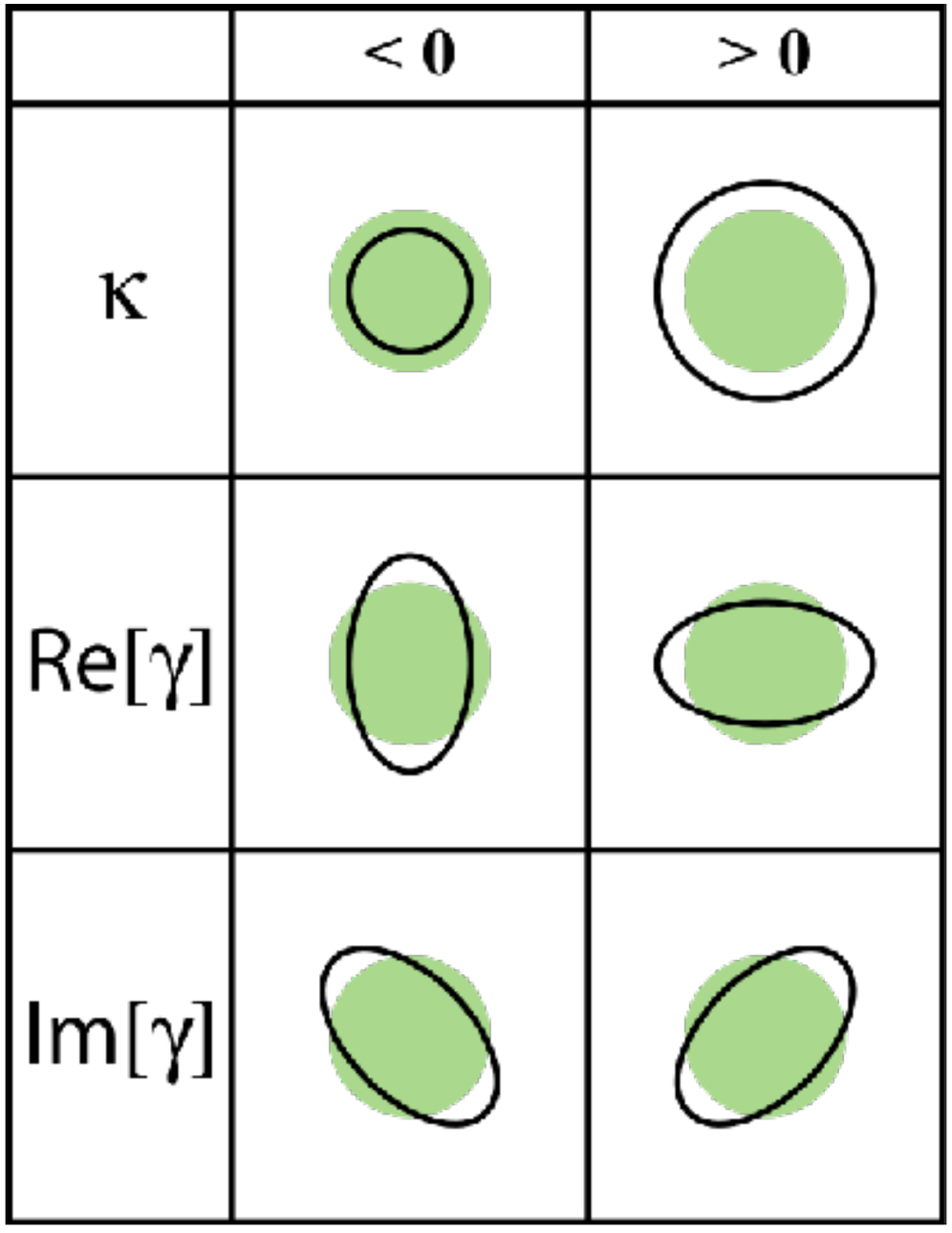

$$g = \frac{\gamma}{1-\kappa}$$

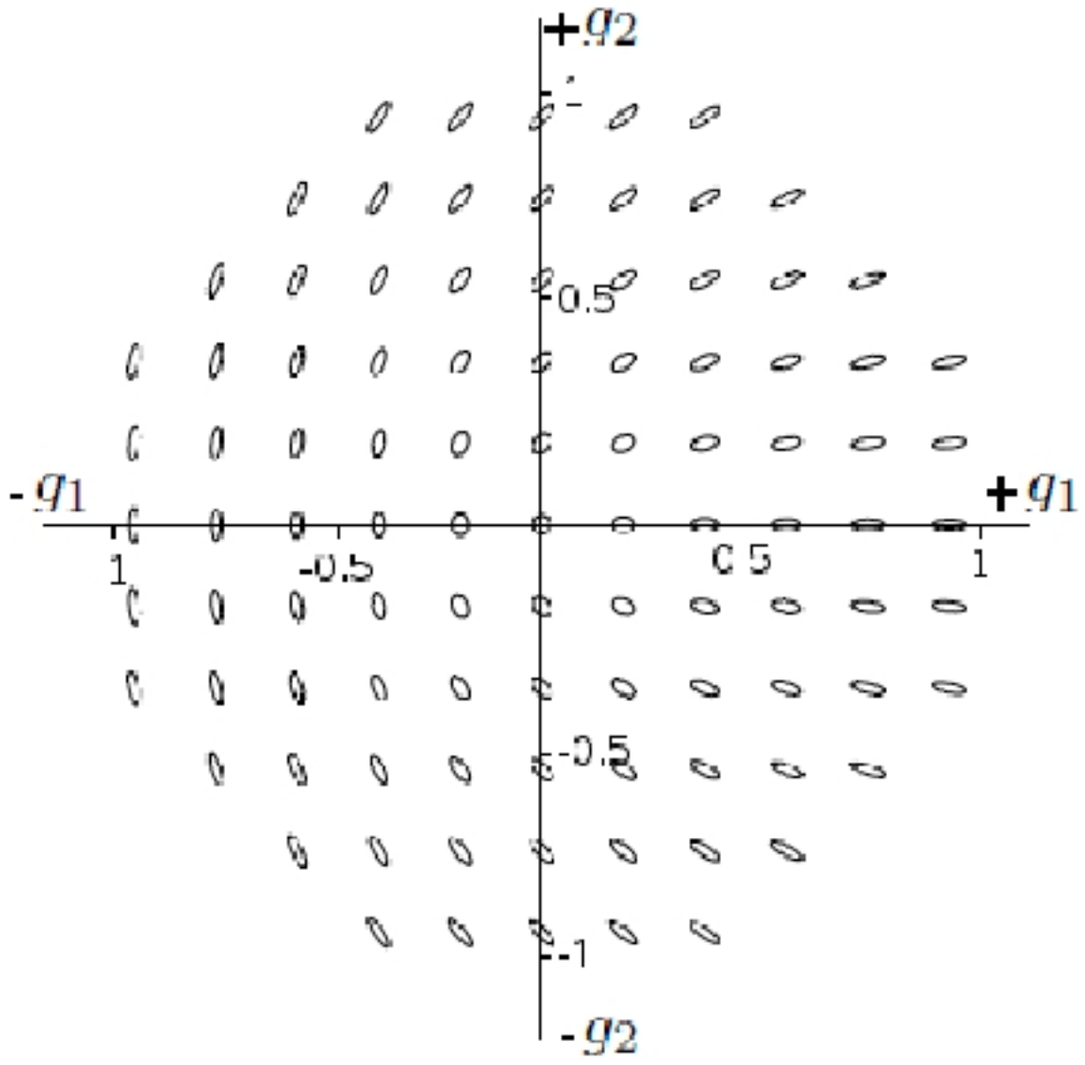

Lensing Equations

Plane transformation for constant κ and γ

Measured distortion: reduced shear $g = \frac{\gamma}{1-\kappa}$

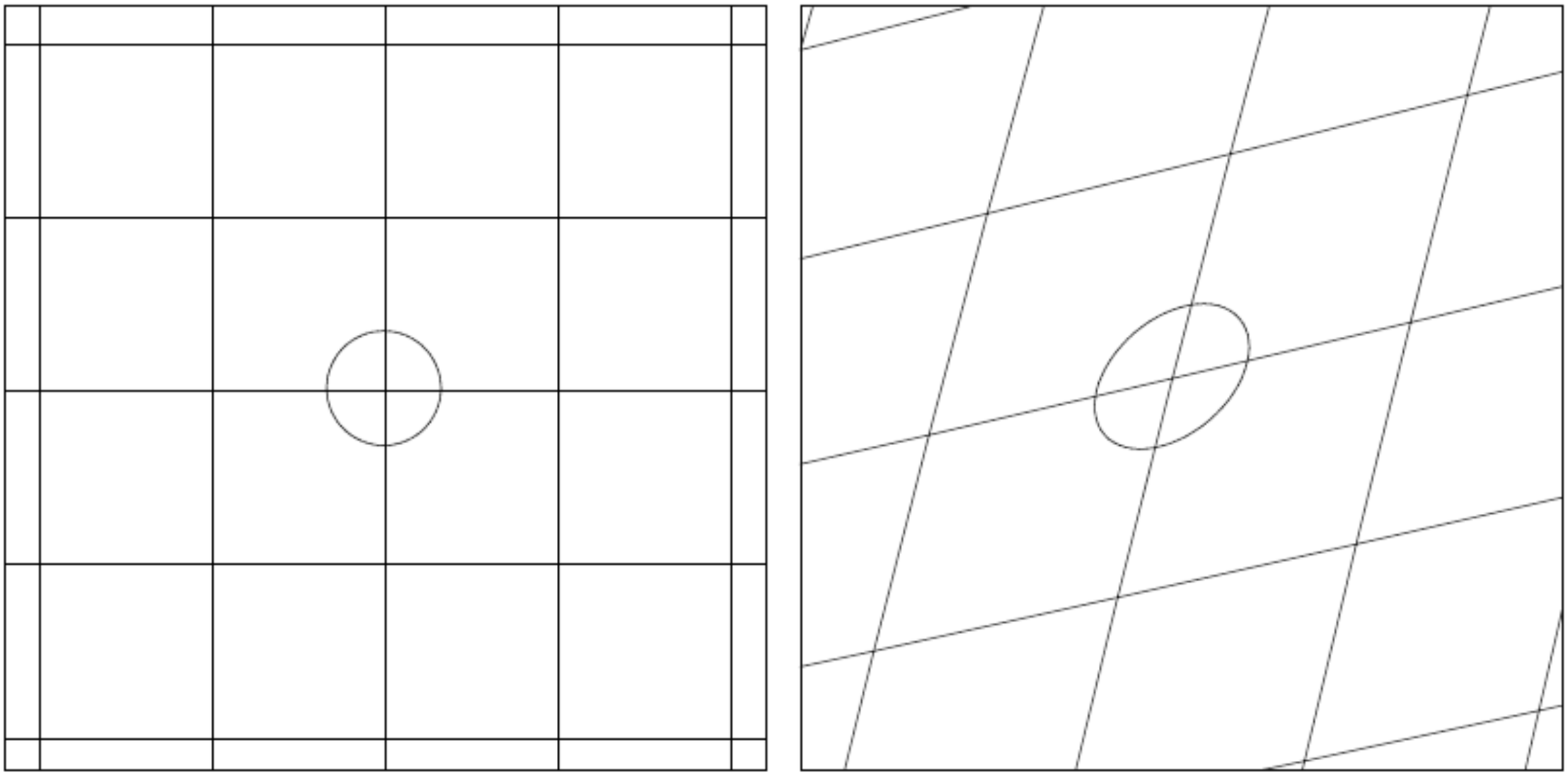

Lensing Equations

Magnification: μ

Size Magnification
=> **Total flux** increase

$$\mu^{-1} = \det(\mathcal{A}^{-1}) = (1-\kappa)^2 - \gamma^2$$

Shear direction is independent of distance parameters:

$$\tan 2\theta_{shear} = \frac{2\partial_{xy}\varphi}{\partial_{yy}\varphi - \partial_{xx}\varphi}$$

Important properties for weak shear analysis &
direction of large arc = direction of the shear

Lensing Equations

Definition: Critical lines

Locus of the image plane where the determinant of the (inverse) magnification matrix is zero:

$$1 - \kappa = \pm\gamma \qquad (\mu = \infty)$$

Critical lines are closed curves and non over-lapping.

In general: 2 types of critical lines:

- tangential (external)
- radial (internal)

Lensing Equations

Definition: Caustic lines

Transform of the critical lines in the source plane;

Caustic lines are delineating the regions with different number of multiple images: crossing a caustic lines adds 2 images

In general: 2 types of caustic lines:

- tangential => diamond shape caustic [astroid]
- radial (usually larger than the tangential one if regular shape)

Lensing Equations

Definition: Caustic lines

Transform of the critical lines in the source plane;

Caustic lines are delineating the regions with different number of multiple images: crossing a caustic lines adds 2 images

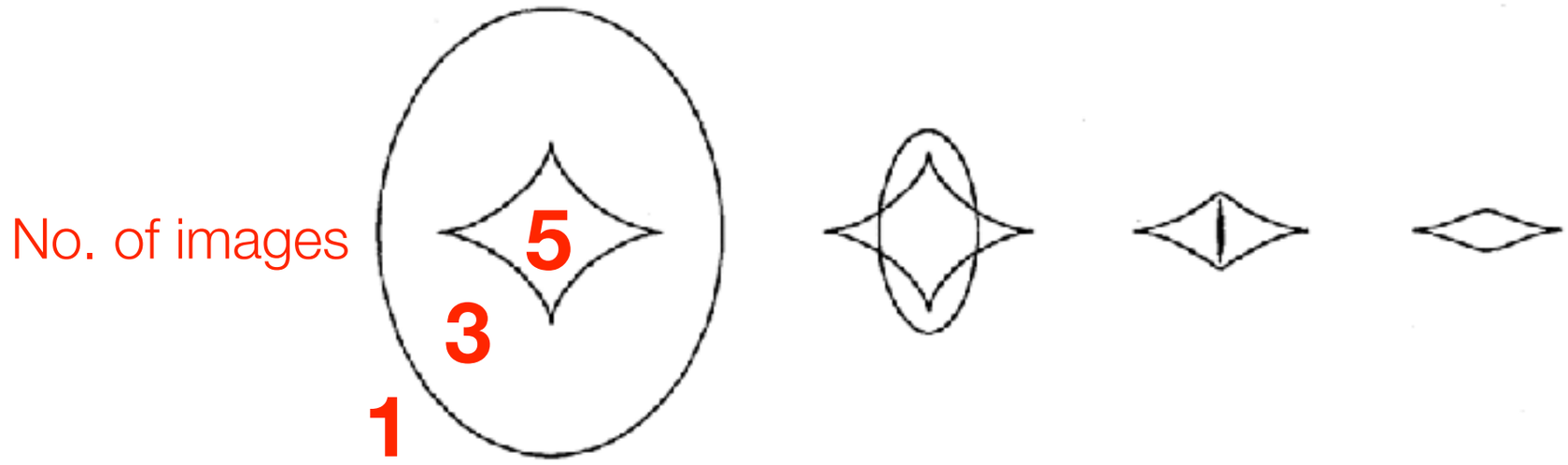

Evolution of the caustic structure with increasing core radius

Lensing theory

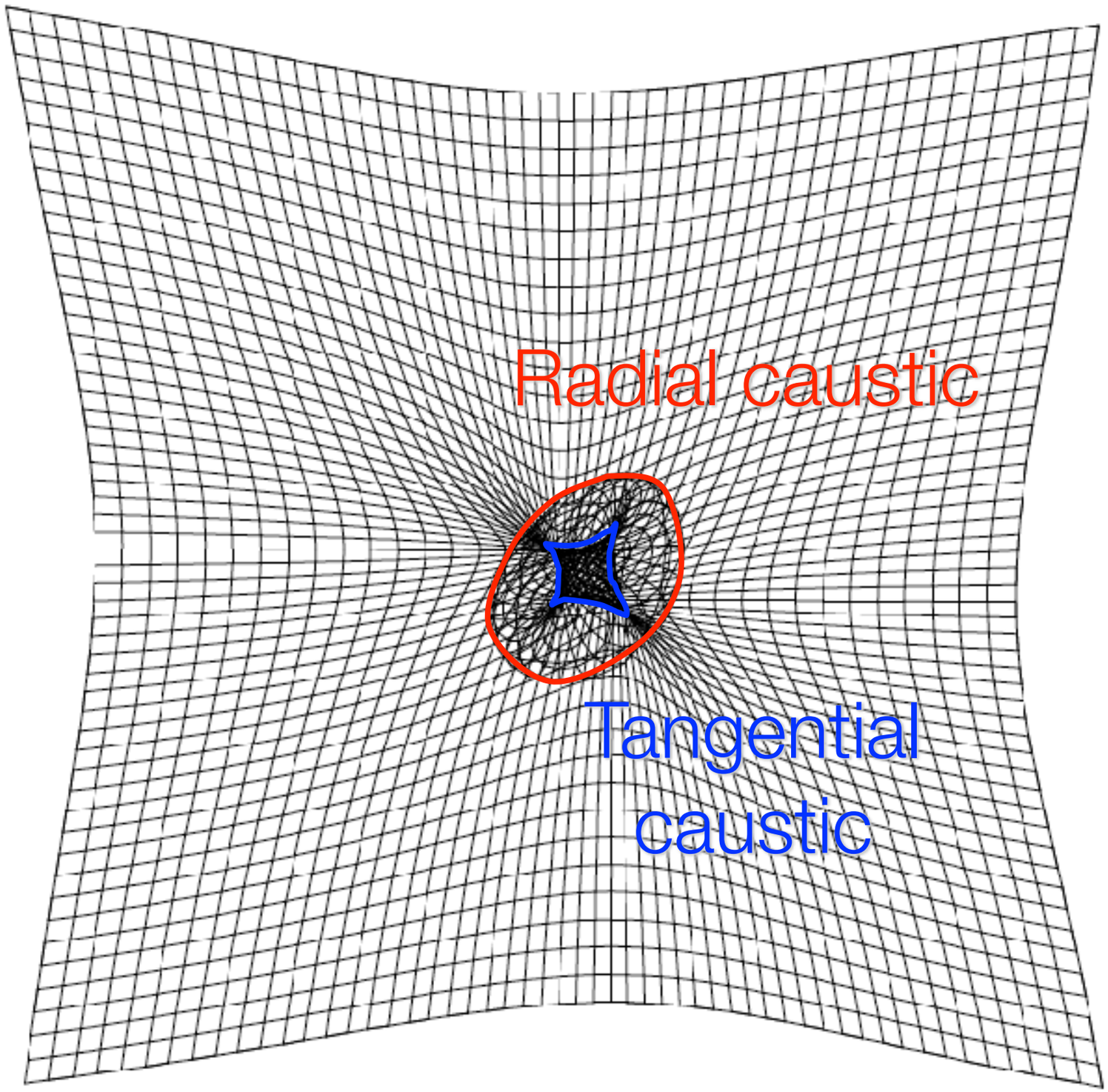

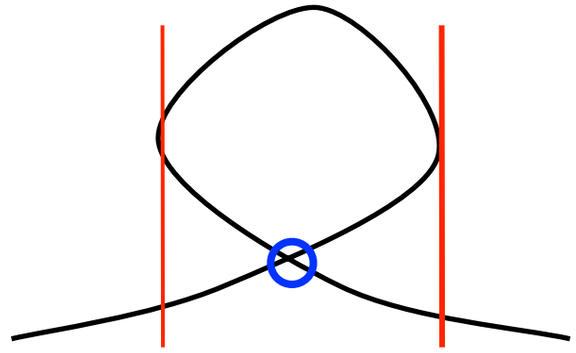

Transform of a regular image plane grid in the source plane

Lensing theory

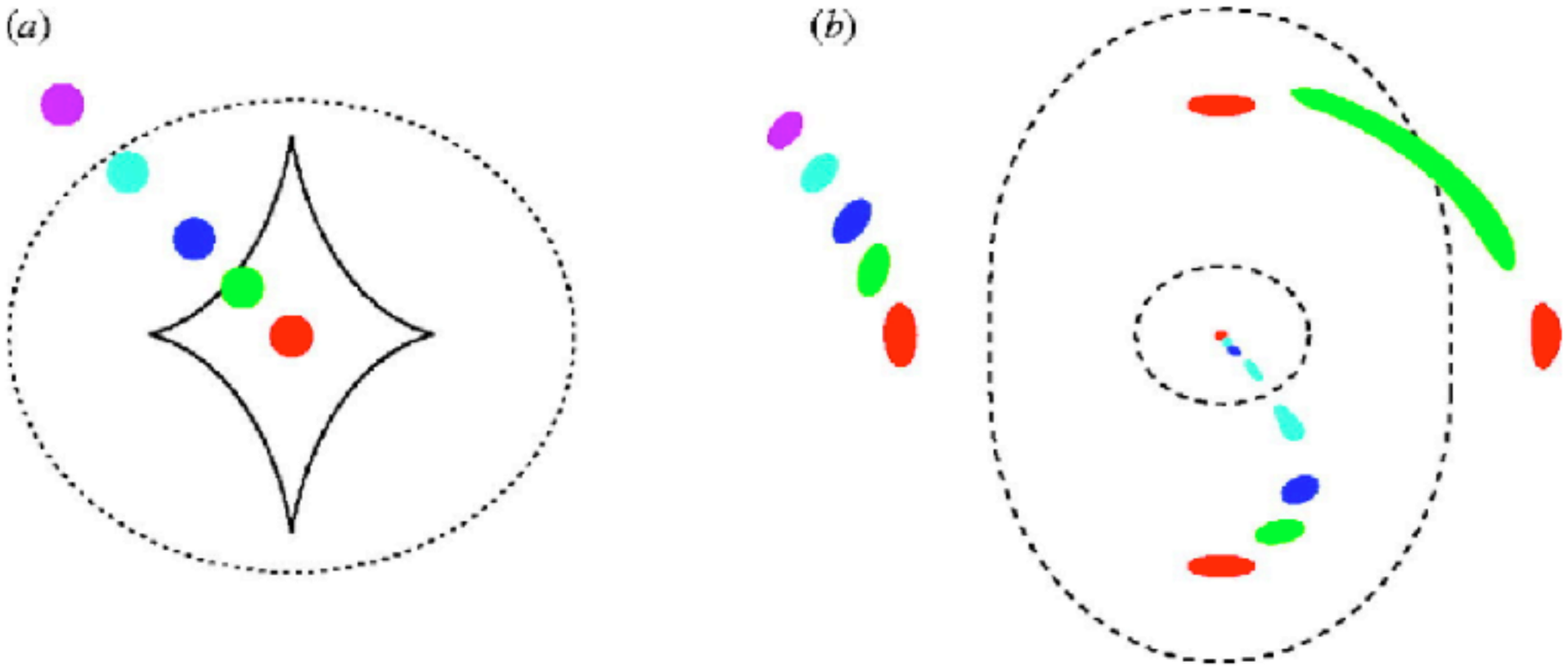

Source plane
caustics

Image plane
critical curves

Lensing Equations

Critical (dashed) and Caustic (solid) Lines

Circular + singular

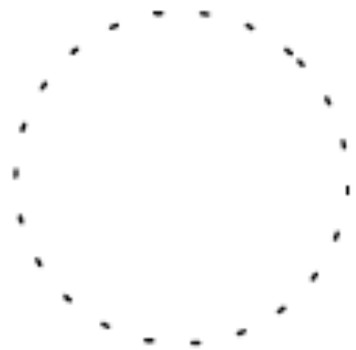

Always 2 images (a)

elliptical + singular

Always 2 images (b)

Circular + non-singular

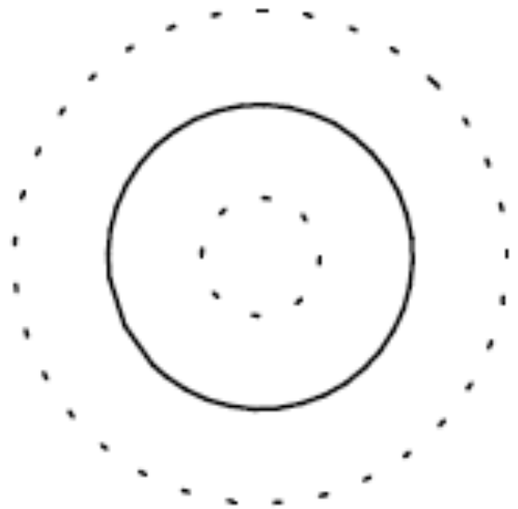

(c)

elliptical + non-singular

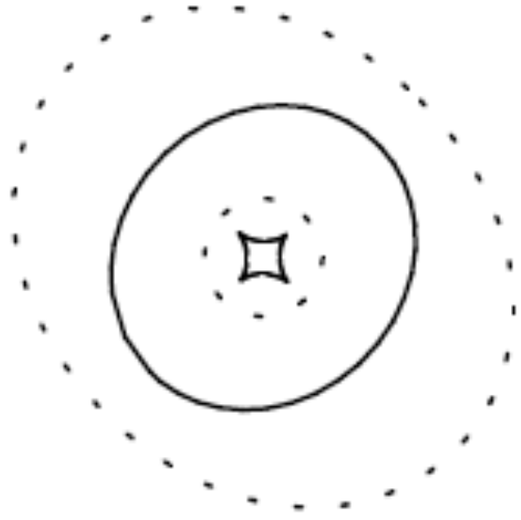

(d)

Bimodal equal-mass

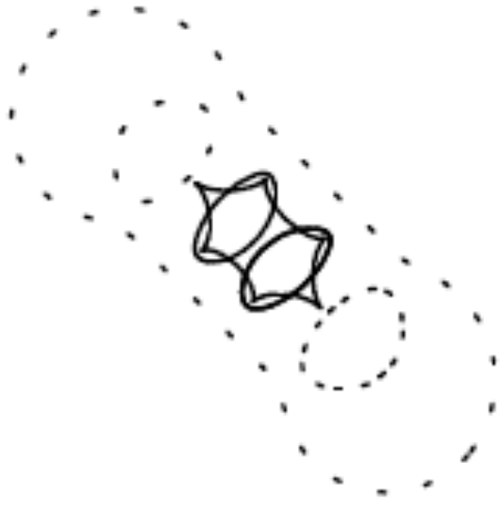

(e)

Bimodal different mass

(f)

Lensing Equations

The case of a circular mass distribution:

Magnification matrix in polar coordinates

$$a^{-1} = \begin{pmatrix} 1 - \partial_{rr}\varphi & 0 \\ 0 & 1 - \frac{1}{r}\partial_r\varphi \end{pmatrix}$$

radial

tangential

$$= \begin{pmatrix} 1 - \partial_r \frac{m(<r)}{r} & 0 \\ 0 & 1 - \frac{m(<r)}{r^2} \end{pmatrix}$$

The tangential caustic is reduced to a point

Tangential arc probe mass
Radial arcs probe mass profile

Lensing equations

Critical line for power-law mass profile $\Sigma \propto \frac{1}{r^\beta}$

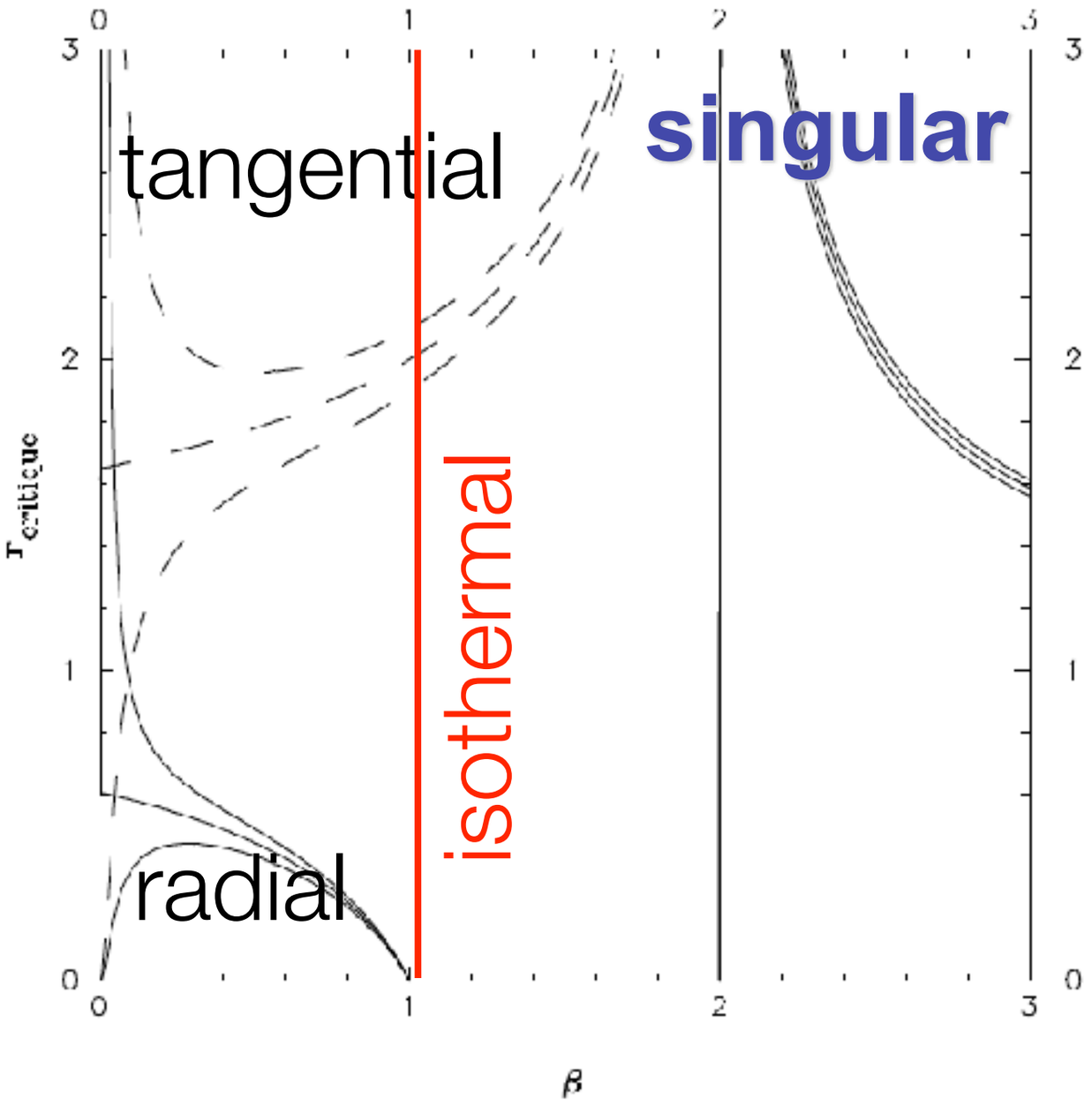

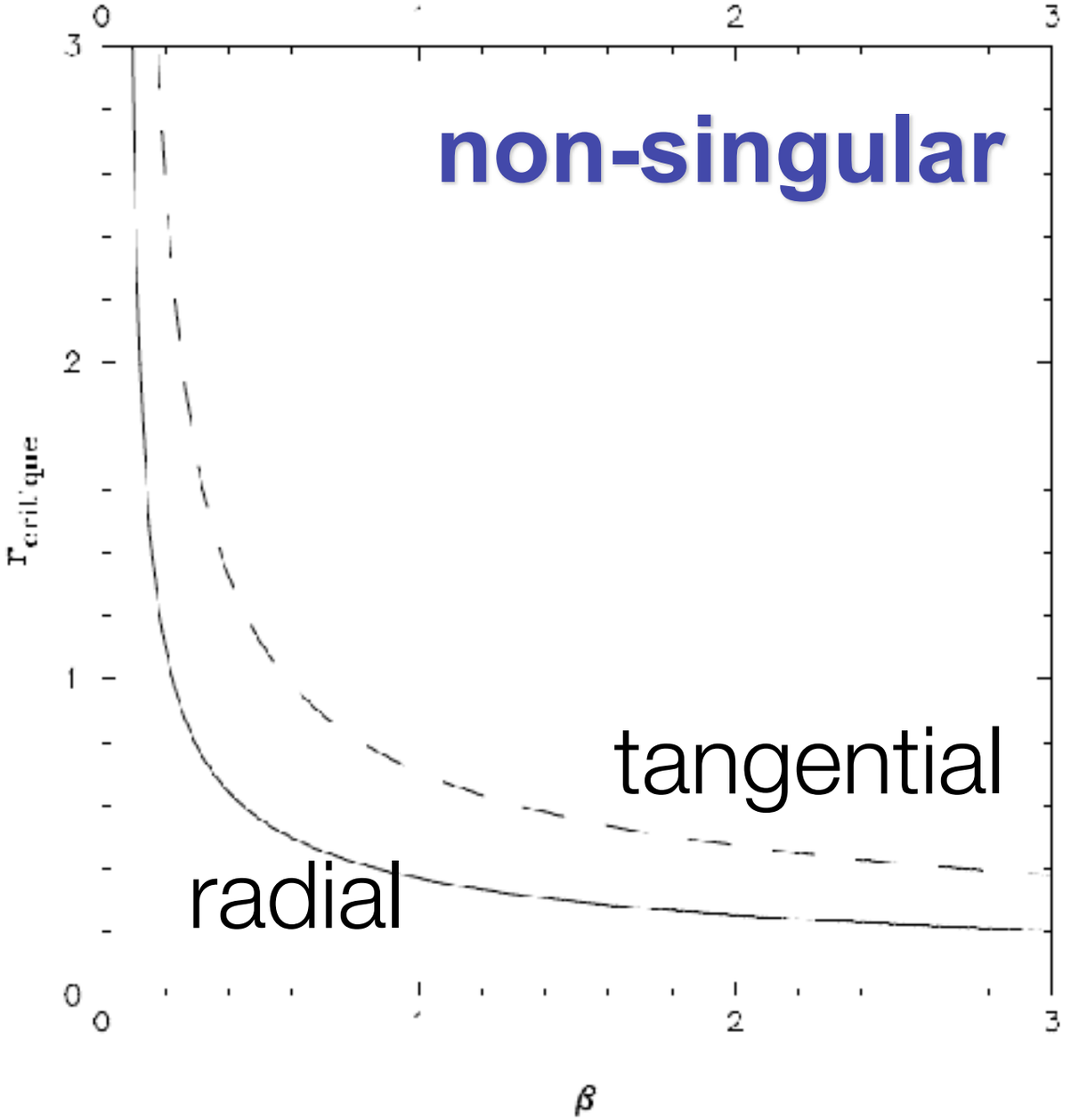

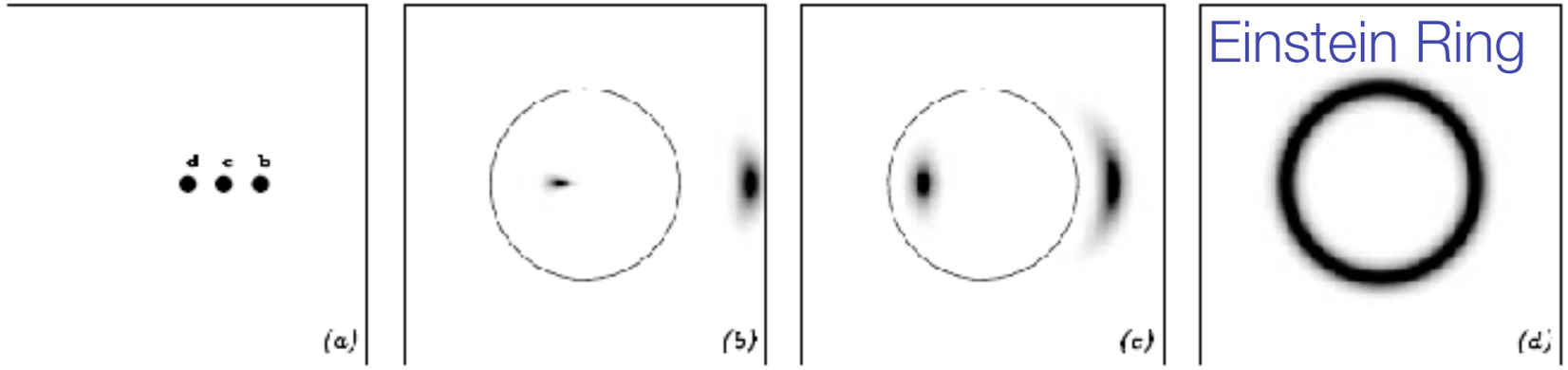

Circular+Singular Mass

Lensing Theory

Elliptical+Singular Mass

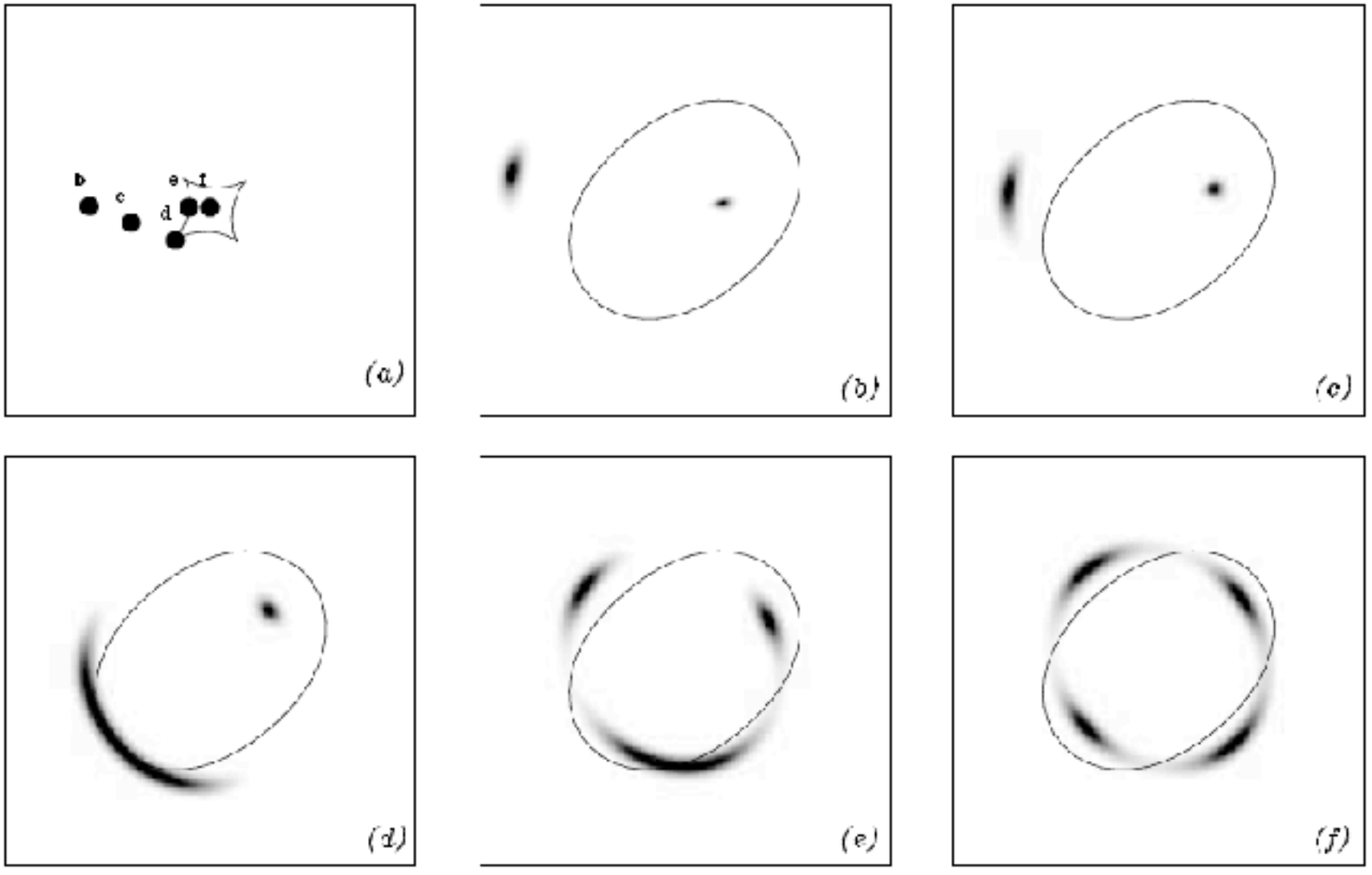

Multiple image configurations for a *singular circular and elliptical mass distribution*

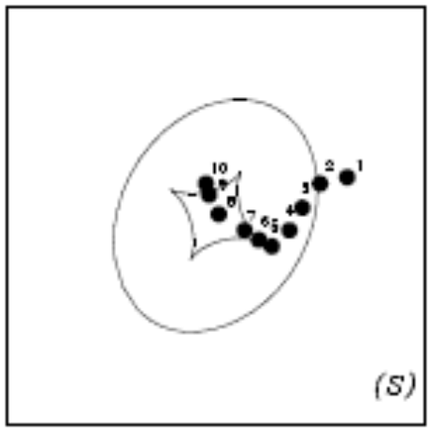

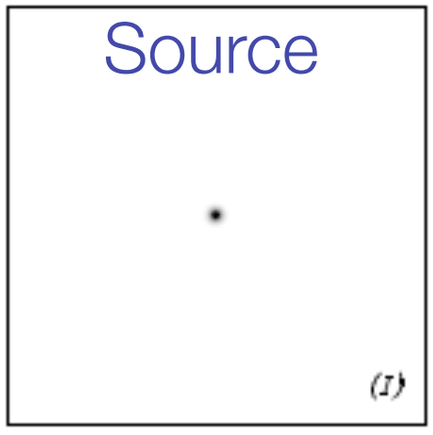

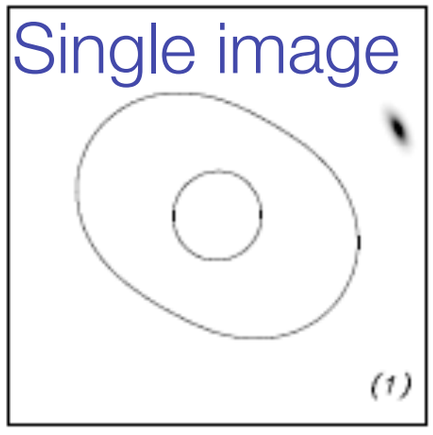

Lensing Theory

Multiple image configurations for a *non-singular elliptical mass distribution*

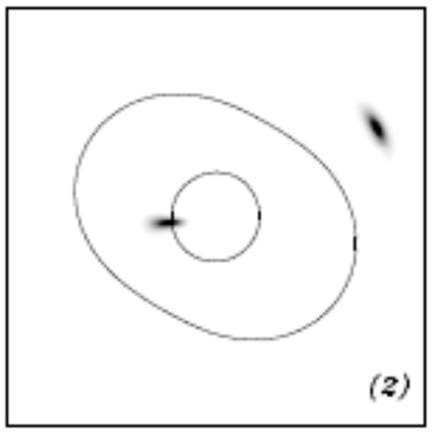

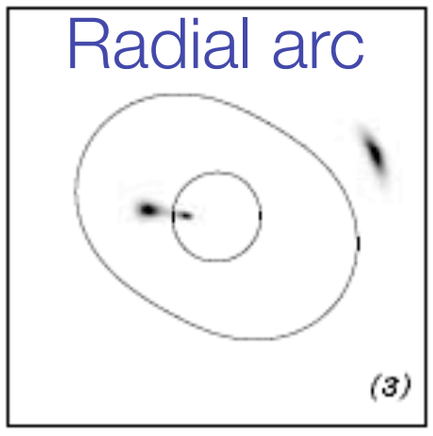

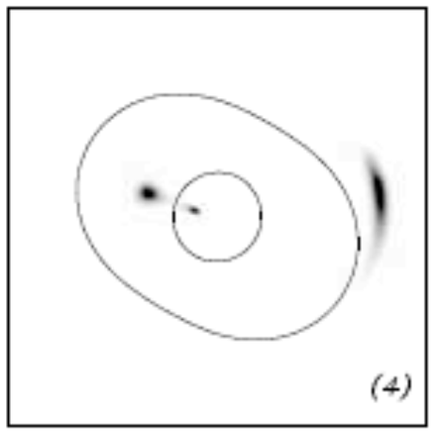

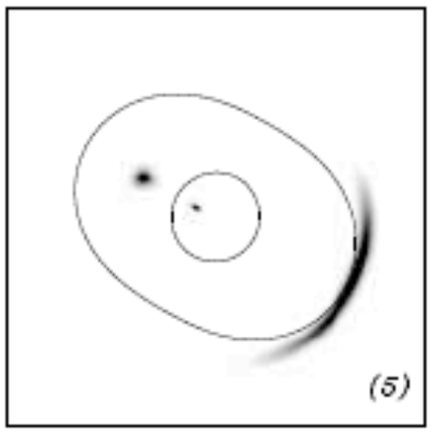

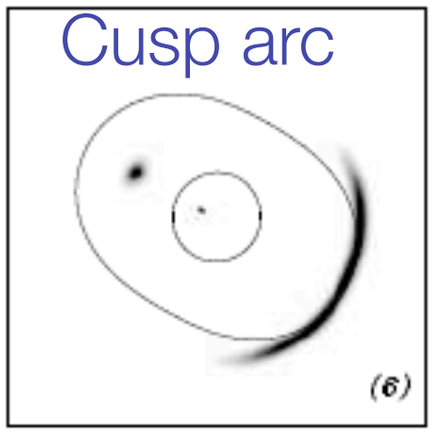

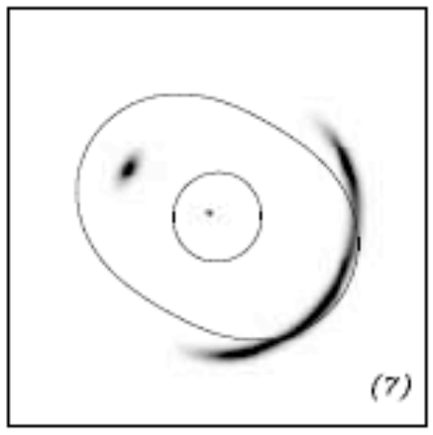

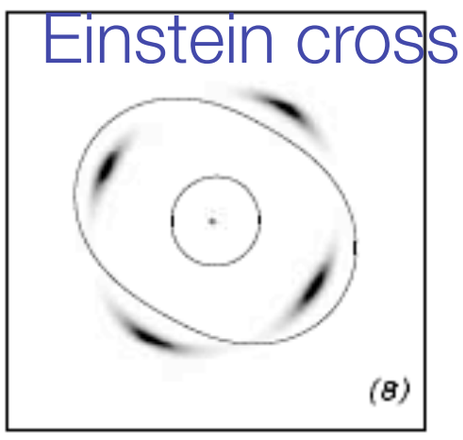

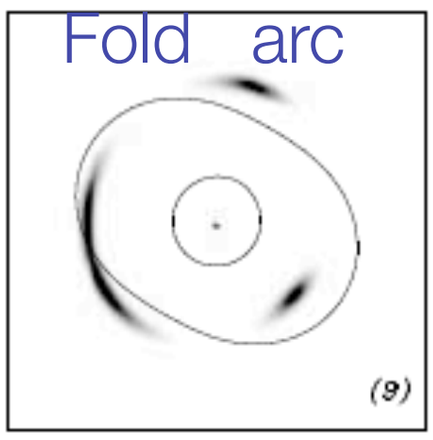

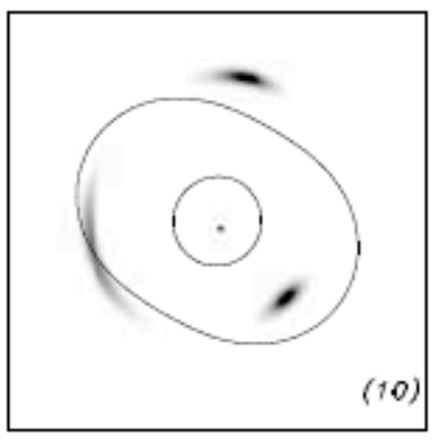

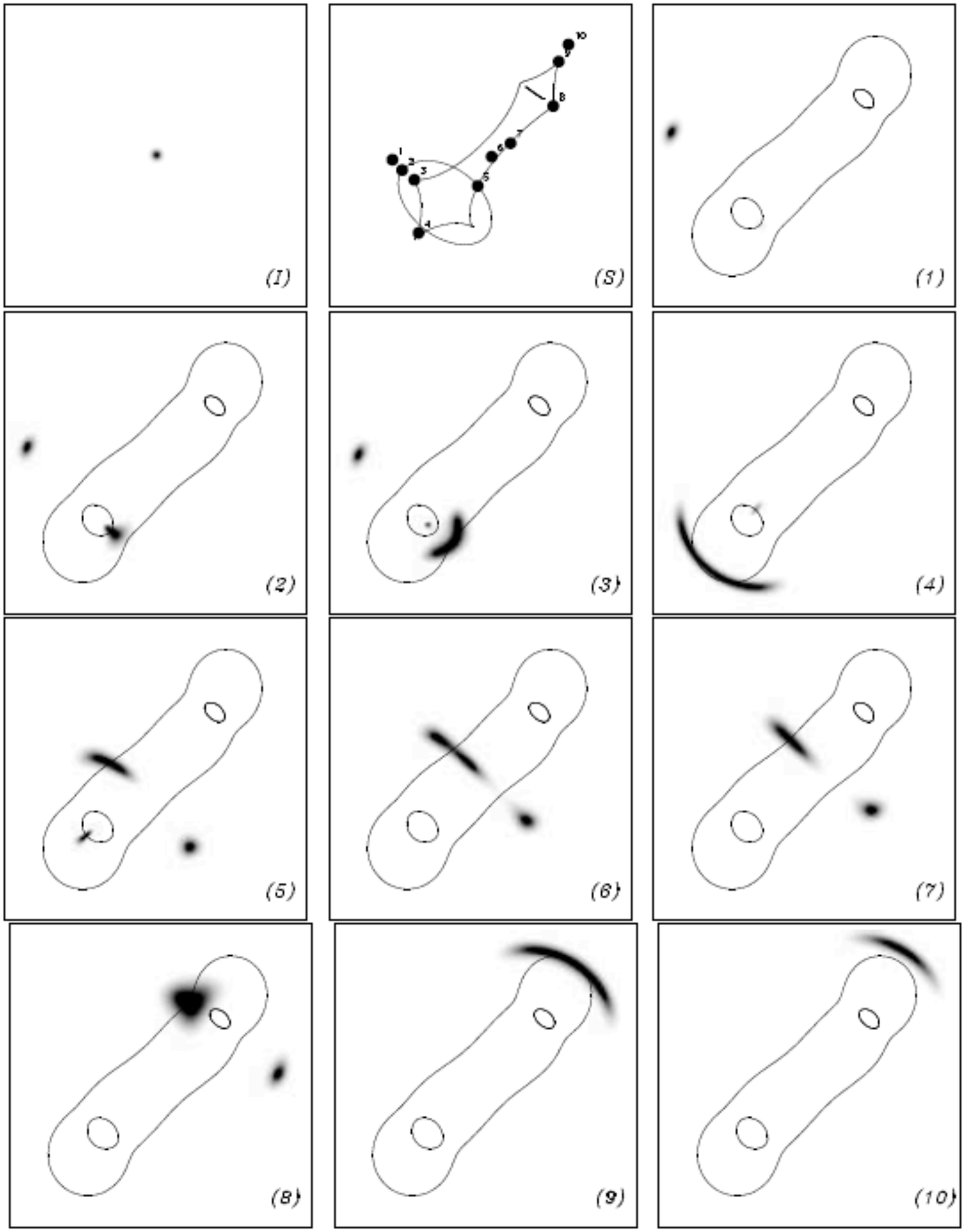

Lensing Theory

Multiple image configurations for a *bimodal mass distribution with similar mass clumps*

Lensing Theory

Multiple image region for:

Circular Elliptical Bimodal

mass distribution

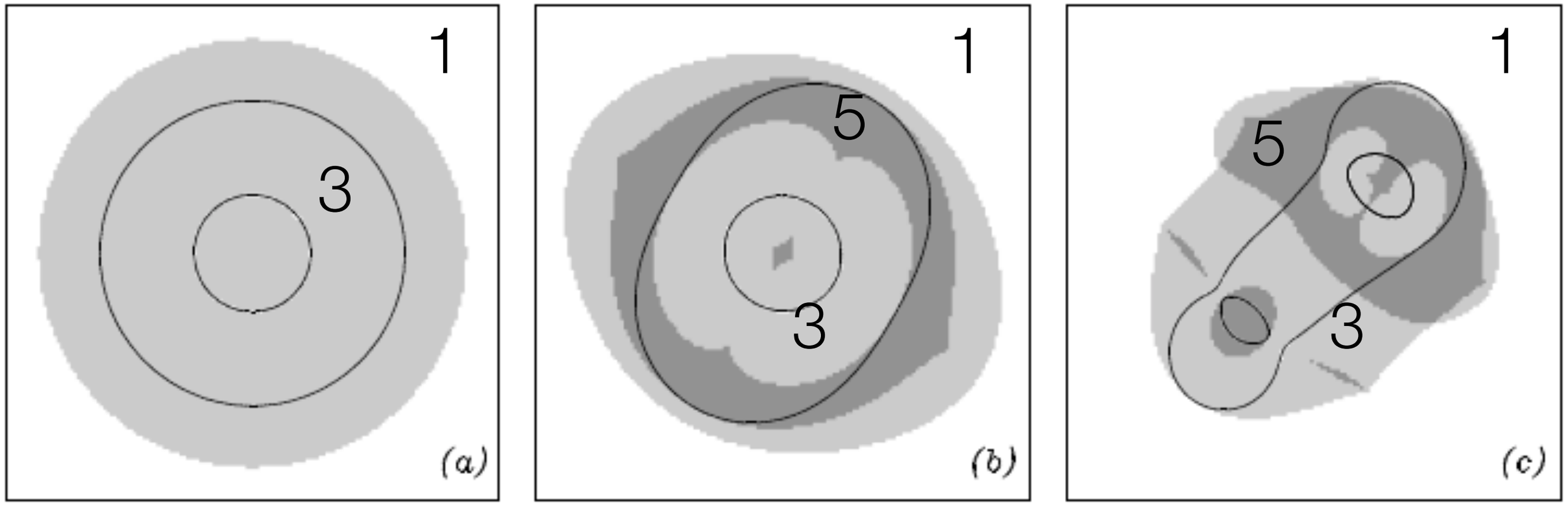

Lensing Theory

Amplification map for:

Circular Elliptical Bimodal

mass distribution

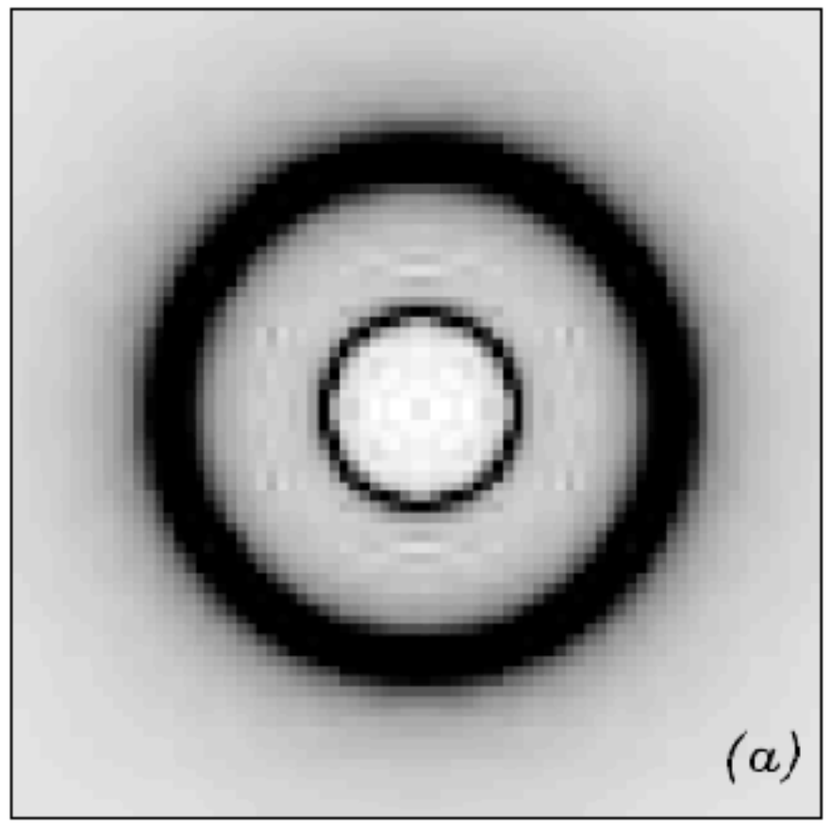

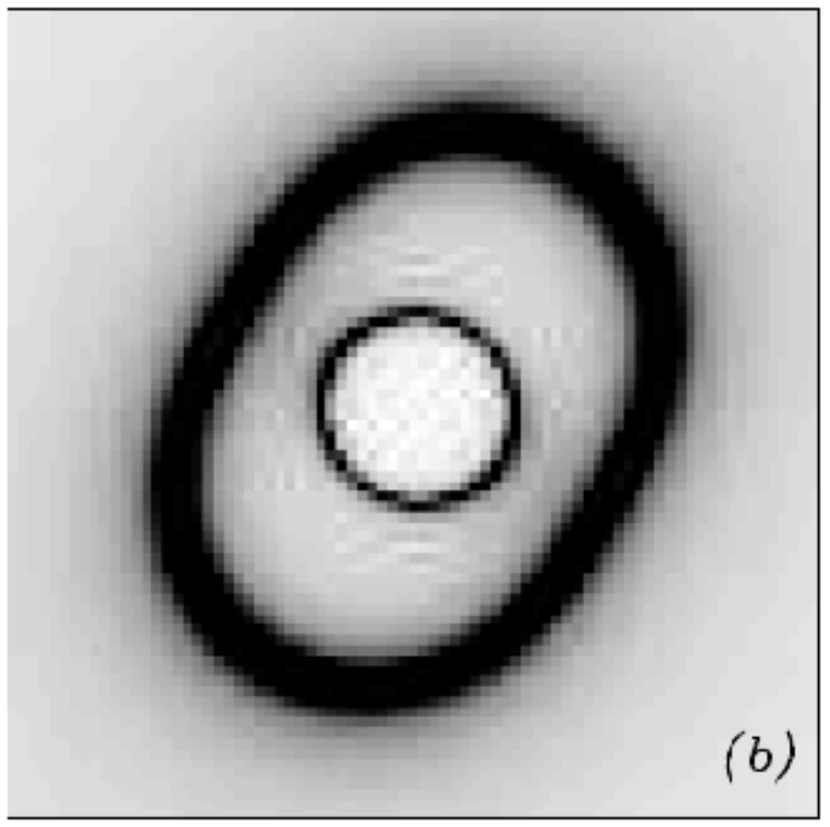

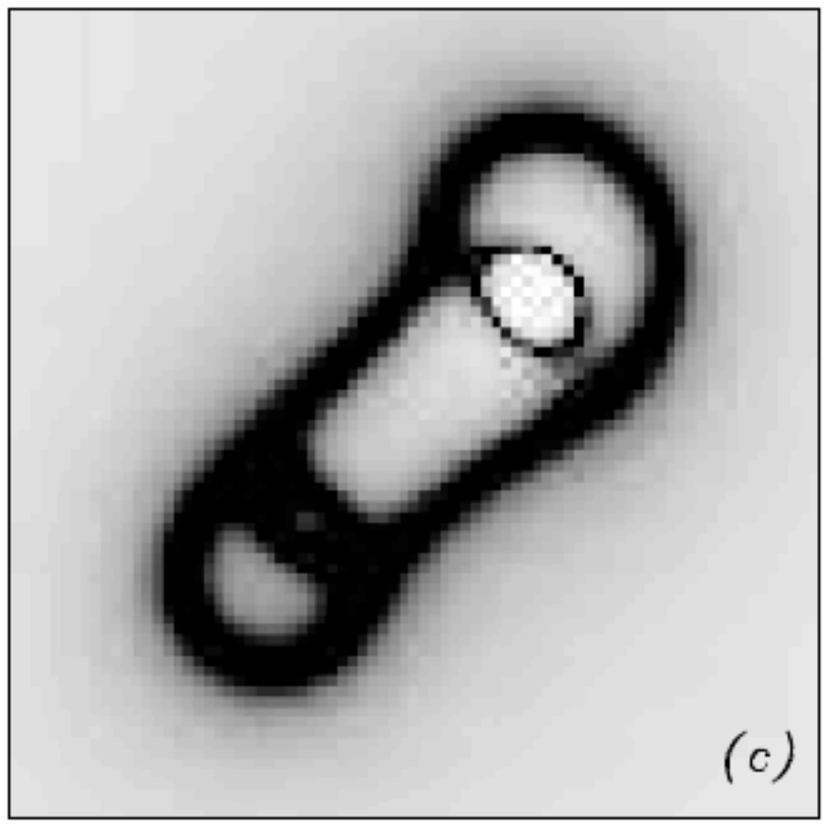

Lensing Theory

Shear field for:

Circular Elliptical Bimodal

mass distribution

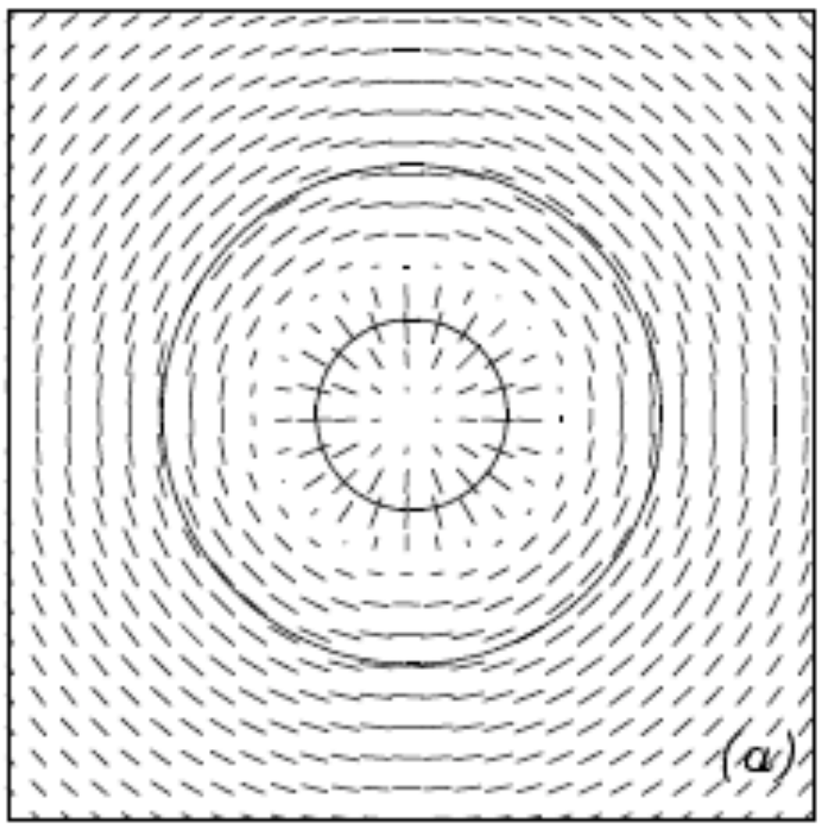

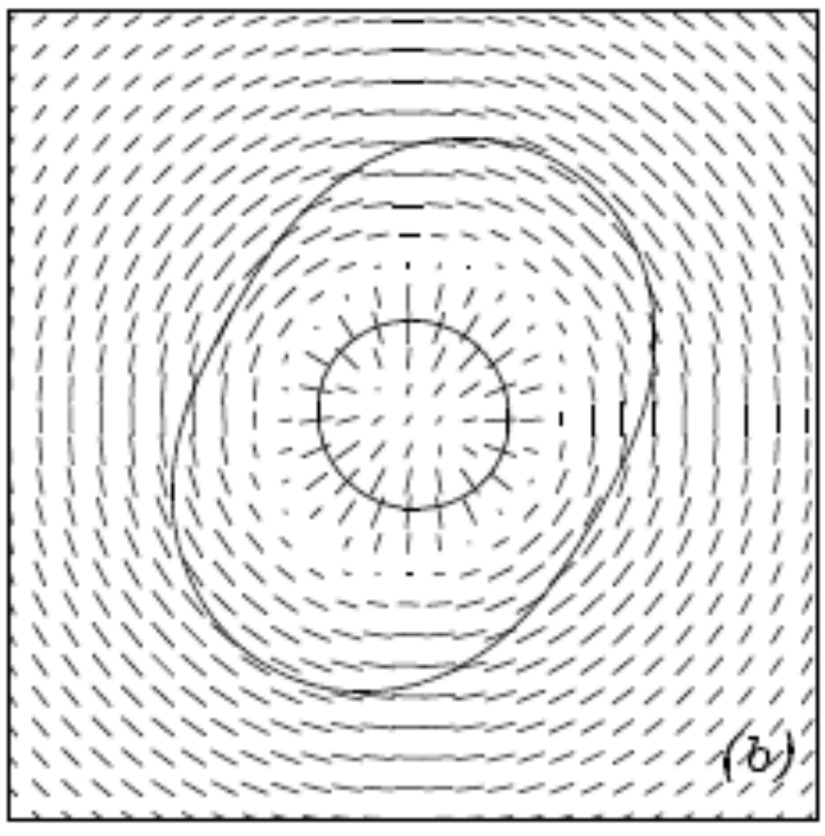

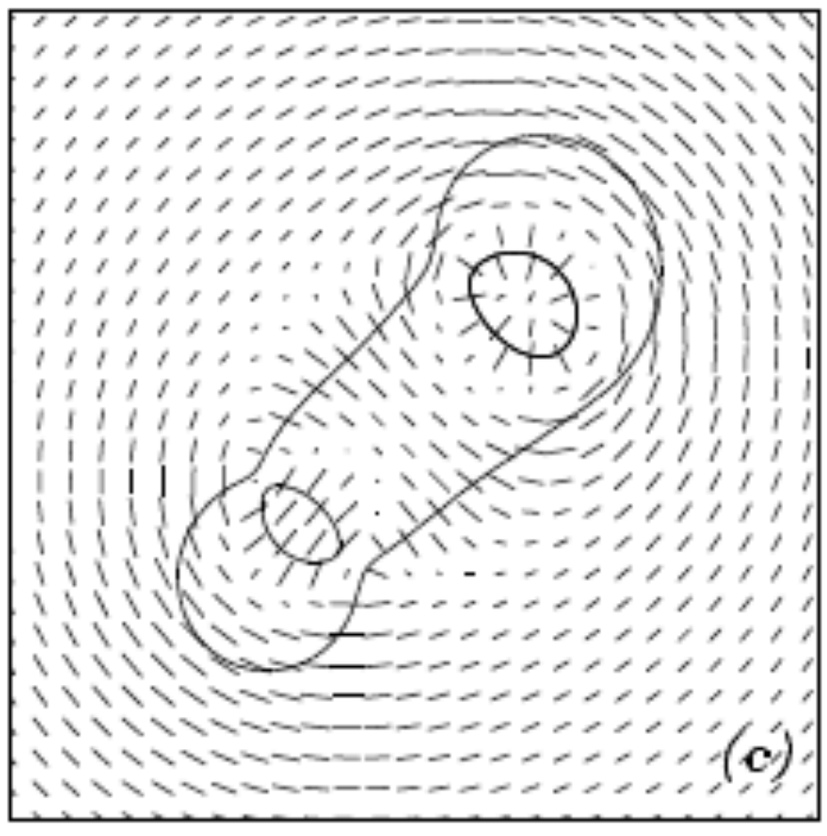

logy

Strong Lensing

Schematic of image fusion on the critical line

Magnification is due to stretching of the image:
surface brightness is conserved through lensing

Strong Lensing

Image parity

Elliptical case

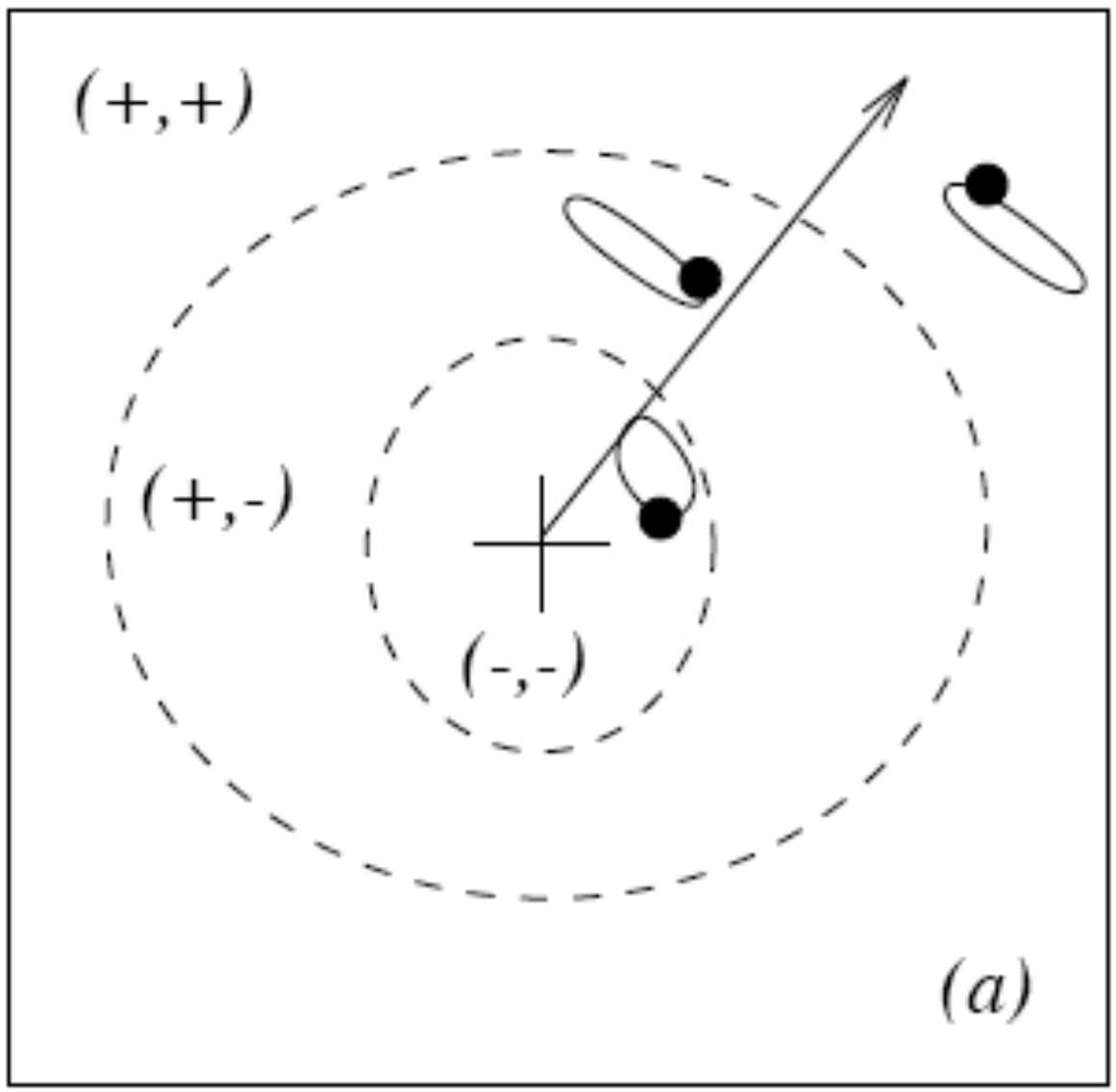

Bimodal case

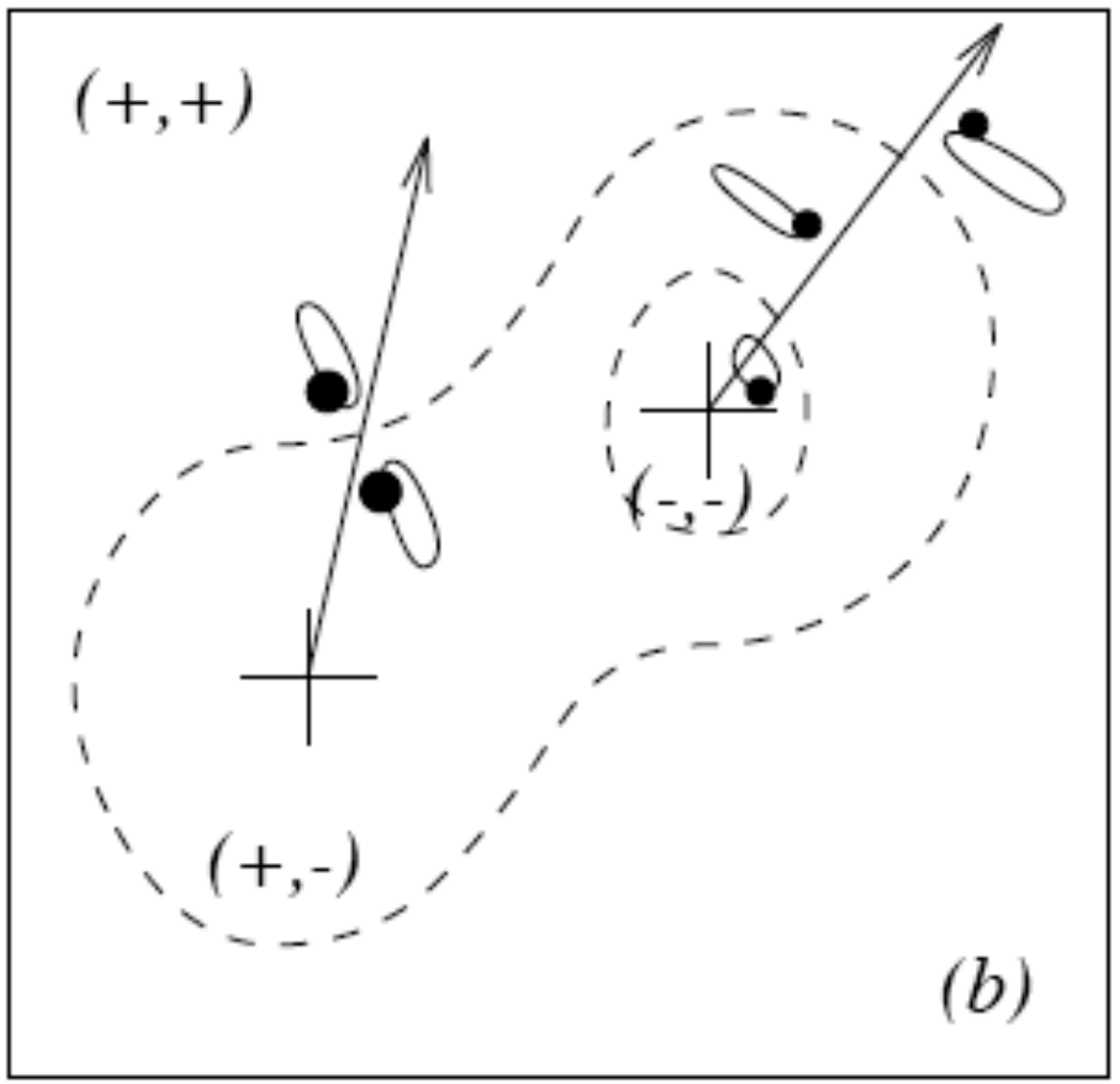

Mass & Einstein Radius

Mass within the Einstein ring:

- mass as a function of lensing potential (circular case): $M(r) = \frac{c^2}{4G}\frac{D_{OS}D_{OL}}{D_{LS}} r\partial_r\varphi(r)$

- Mass within the tangential critical line (Einstein ring):

$$M(r_E) = \pi\Sigma_{crit} r_E^2$$

$$\approx 1.1 \times 10^{14}\, M_\odot \left(\frac{\theta_E}{30''}\right)^2 \left(\frac{D}{1\,\mathrm{Gpc}}\right)$$

- Value of Einstein radius is not everything! Anisotropy is also very important.

Micro-Lensing

Micro Lensing

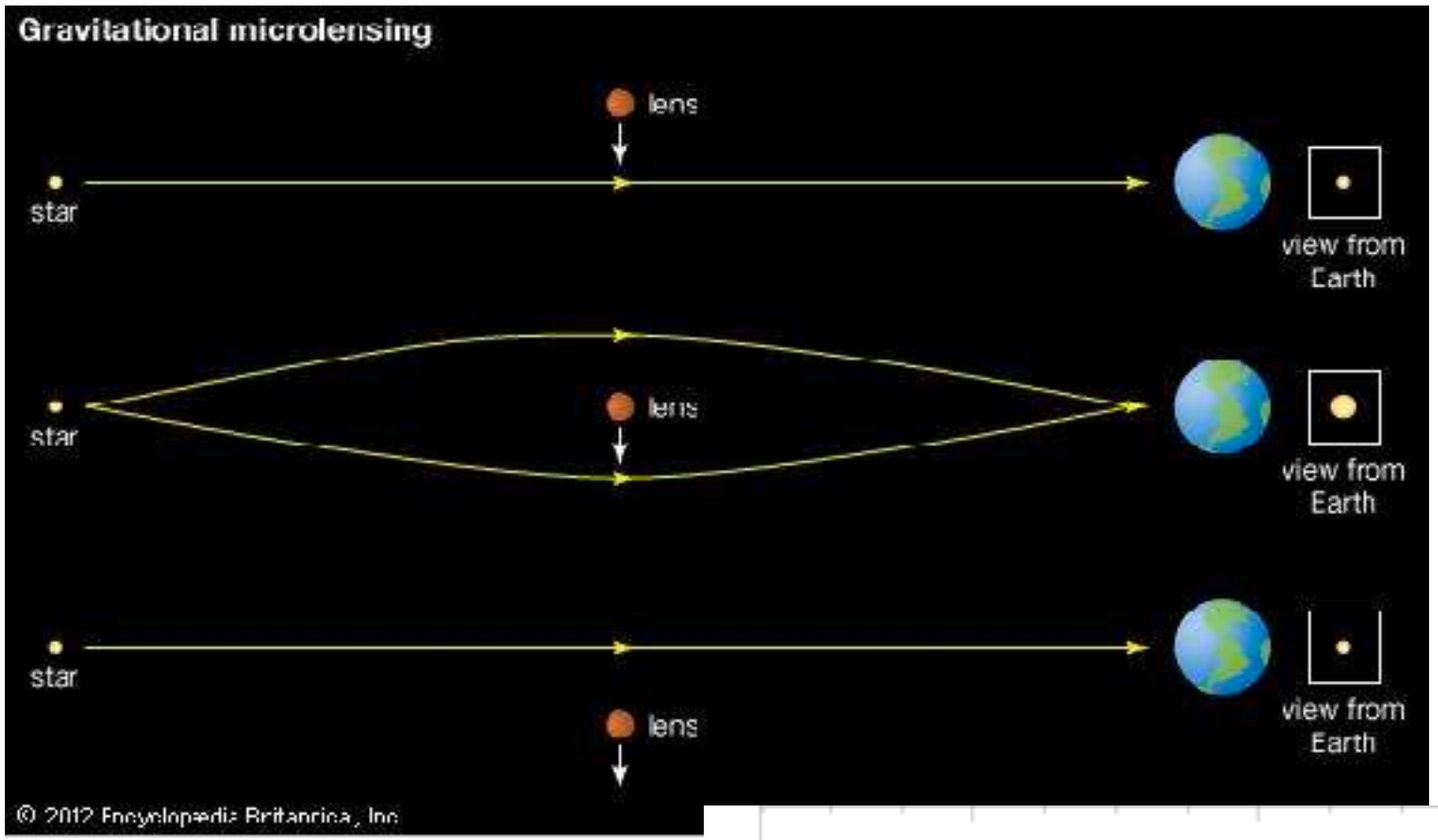

- Moving object lensing a distant star
- Achromatic effect
- search for DM in compact form (EROS, MACHO, OGLE projects)

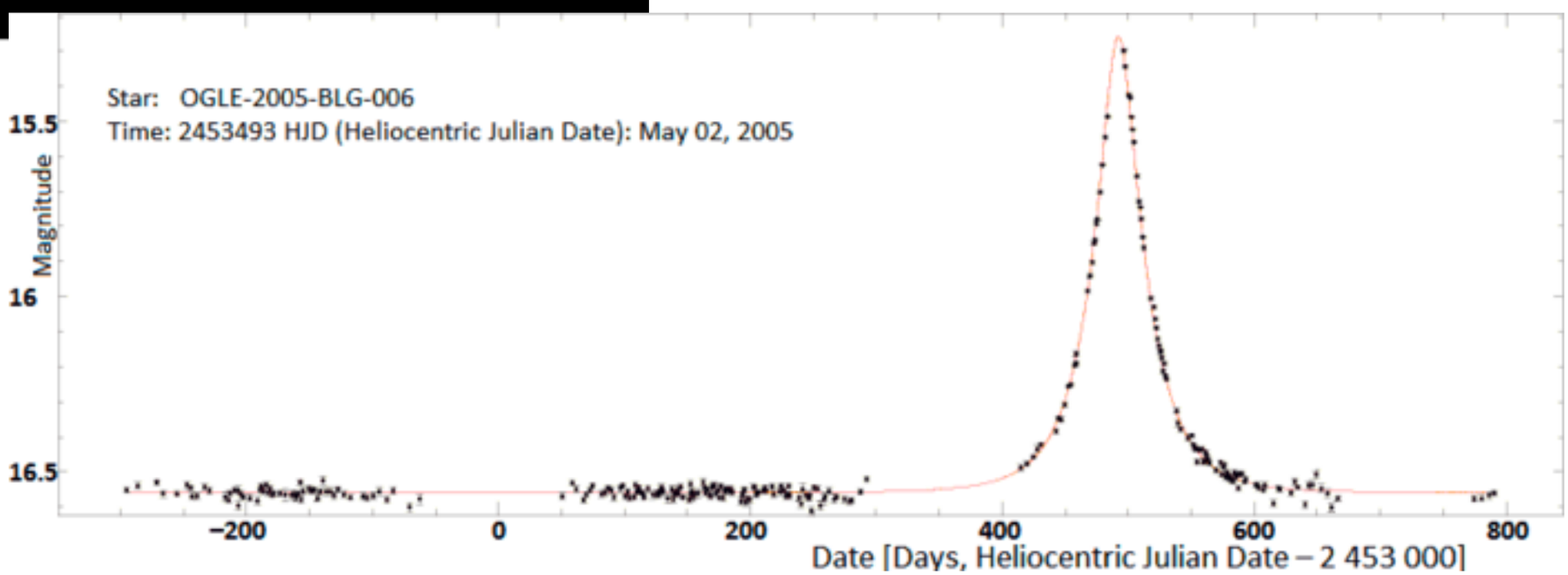

Halo Dark Matter & Paczynski's Idea

(Paczynski 1986)

- 20~40 times more dark matter than visible mass.
- MAssive Compact Halo Objects (MACHOs) ←→ WINPs

- MACHO can be observed by Microlensing.
- $\tau \sim 10^{-6}$ → need to observe 1M stars !

Constraints on the fraction of DM as compact object (BH)

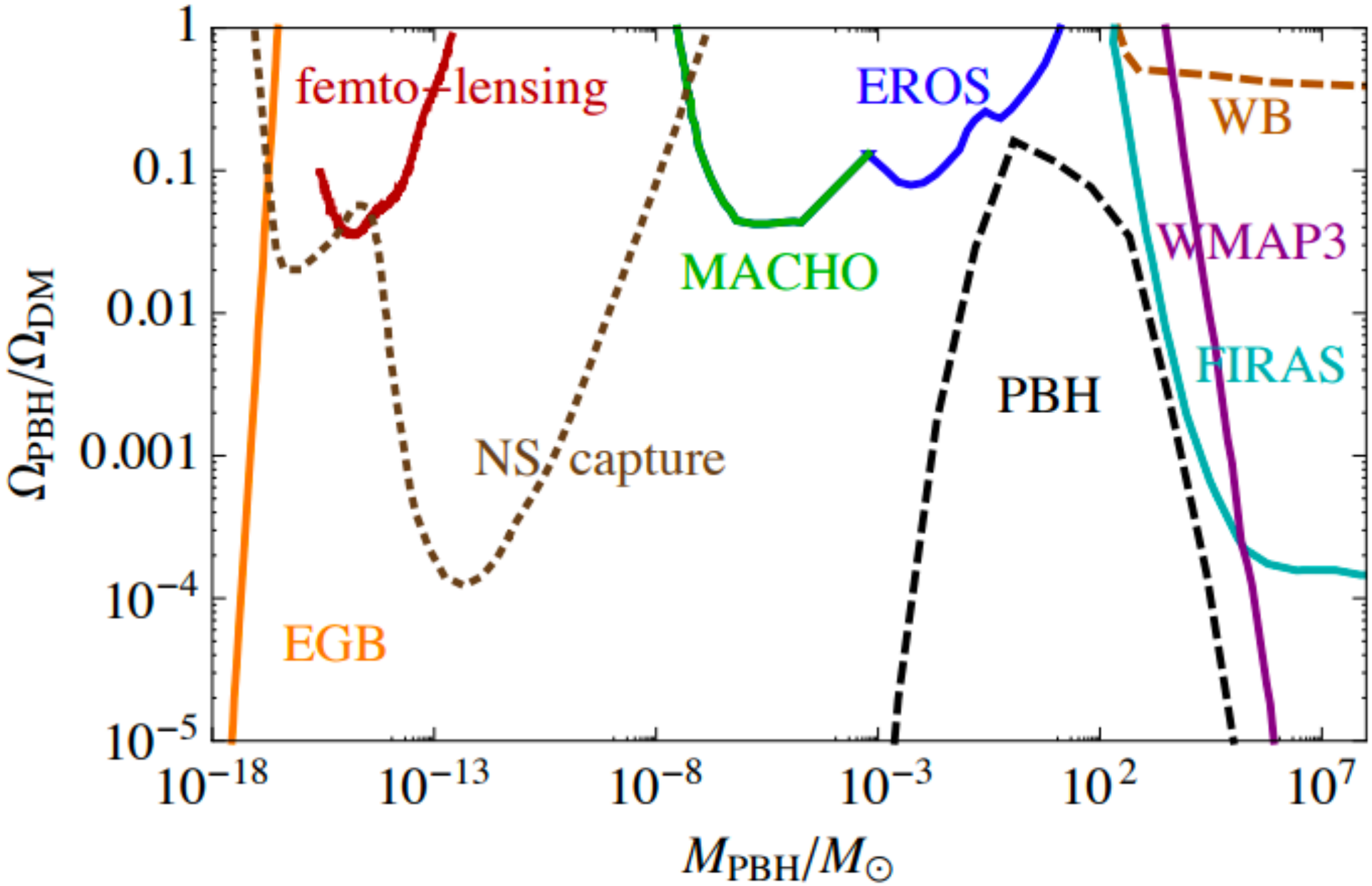

Garcia-Bellido et al 2017

Micro Lensing by exo-planets